

# A LEAST-SQUARES APPROXIMATION METHOD FOR THE TIME-HARMONIC MAXWELL EQUATIONS

JAMES H. BRAMBLE, TZANIO V. KOLEV, AND JOSEPH E. PASCIAK

ABSTRACT. In this paper we introduce and analyze a new approach for the numerical approximation of Maxwell’s equations in the frequency domain. Our method belongs to the recently proposed family of negative-norm least-squares algorithms for electromagnetic problems which have already been applied to the electrostatic and magnetostatic problems as well as the Maxwell eigenvalue problem (see [5, 4]). The scheme is based on a natural weak variational formulation and does not employ potentials or “gauge conditions”. The discretization involves only simple, piecewise polynomial, finite element spaces, avoiding the use of the complicated Nédélec elements. An interesting feature of this approach is that it leads to simultaneous approximation of the magnetic and electric fields, in contrast to other methods where one of the unknowns is eliminated and is later computed by differentiation. More importantly, the resulting discrete linear system is well-conditioned, symmetric and positive definite. We demonstrate that the overall numerical algorithm can be efficiently implemented and has an optimal convergence rate, even for problems with low regularity.

## 1. INTRODUCTION

The numerical simulation of electromagnetic phenomena is of critical importance in many practical applications, including the design of various devices such as antennas, radar, microwaves, waveguides and particle accelerators, cf. [18, 28, 27]. Many of the current discretization methods for these problems are based on the complicated edge elements introduced by Nédélec and result in a linear system that is difficult to precondition. In this paper we present a different approximation technique which involves only simple, piecewise polynomial finite elements and standard preconditioners for second order elliptic problems.

Let  $\Omega \subset \mathbb{R}^3$  be a bounded open set. We choose to concentrate on three-dimensional domains, but our results carry over to simpler, two-dimensional problems. Details illustrating this are given in Section 4.

---

Received by the editor June 15, 2005.

1991 *Mathematics Subject Classification.* 78M10, 65F10, 65N30.

*Key words and phrases.* Maxwell’s equations, finite element approximation, negative-norm least-squares, div-curl systems, Maxwell eigenvalues.

This work was performed under the auspices of the U.S. Department of Energy by University of California Lawrence Livermore National Laboratory under contract No. W-7405-Eng-48. Additional support was provided by the National Science Foundation grant No. 0311902.

Let  $\mathbf{n}$  be the outward unit normal on  $\partial\Omega$ <sup>1</sup>. The time-harmonic Maxwell equations are given by

$$(1.1) \quad \begin{cases} \nabla \times \mathbf{h} = \lambda \varepsilon \mathbf{e} + \mathbf{j} & \text{in } \Omega, \\ \nabla \times \mathbf{e} = -\lambda \mu \mathbf{h} + \mathbf{m} & \text{in } \Omega, \\ \mu \mathbf{h} \cdot \mathbf{n} = 0 & \text{on } \partial\Omega, \\ \mathbf{e} \times \mathbf{n} = \mathbf{0} & \text{on } \partial\Omega, \end{cases}$$

where the unknowns,  $\mathbf{h}$  and  $\mathbf{e}$ , are complex vector fields defined on  $\Omega$  and corresponding to the magnetic and electric parts of the electromagnetic field. The fields  $\mathbf{j}$  and  $\mathbf{m}$  are given data representing the source electric and magnetic current densities. The functions  $\varepsilon$  and  $\mu$  describe the experimentally determined material properties, respectively, the magnetic permeability and the electric permittivity. We shall assume that they are real-valued and piecewise constant in this paper. In addition,  $\lambda = -i\omega$ , where  $\omega \in \mathbb{R}$  is the fixed frequency of propagation of the electromagnetic waves. We consider only the simplest boundary conditions which correspond to a region surrounded by a perfect conductor.

There are a variety of methods for approximation of (1.1) and related problems, some of which are discussed in [7, 8, 19, 20]. It is common to use a discretization based on the curl-conforming Nédélec spaces introduced in [21, 22]. Even though the use of edge elements in unstructured computational codes is widespread, cf. [14], their implementation, especially in the higher-order cases, can be challenging. An additional difficulty associated with this approach is that the resulting matrix problem is indefinite, and therefore, the efficient solution of the discrete system presents a serious challenge, although much progress has been made in this direction, see e.g. [15, 17, 26, 16].

Recently, an interior penalty discontinuous Galerkin method was introduced and analyzed in [23]. This method allows for different orders of approximation in the different regions of the grid. The error estimates in this paper were proven only in the case of smooth coefficients. We also note that the resulting bilinear form is quite complicated.

A different approach, proposed in [13], is based on decomposing the solution into regular and singular components. The regular part can be approximated by nodal finite elements while the singular part is treated by adding singular functions to the space. The implementation of this procedure may be quite involved since one needs to deal explicitly with the singular functions. Many other alternatives, such as mortar and FETI methods applied to the Maxwell's equations [3, 29], have been proposed. Adaptive *hp* solvers have also been investigated, see [12].

The idea that we introduce in this paper is different from the above-mentioned algorithms since its implementation requires only piecewise polynomial finite element spaces. It is based on a very weak variational formulation of the time-harmonic Maxwell equations, similar to the method for the electrostatic and magnetostatic div-curl systems presented in [5]. There is also a natural connection to the eigenvalue problem which was studied in [4]. Our approximation is based in  $\mathbf{L}^2(\Omega)$  and is therefore applicable to many practical problems where the solution fields have low regularity. An additional advantage of the method is that it directly and simultaneously approximates the variables of interest (the electric *and* magnetic fields), avoiding potentials, “gauge conditions” and numerical differentiation. The discretization is based on a negative-norm least-squares

---

<sup>1</sup>We employ the usual convention of using boldface symbols to denote vector quantities

method which can be efficiently implemented using preconditioners for standard second order elliptic problems. The resulting discrete system is uniformly equivalent (independent of the mesh size) to the mass matrix in  $\mathbf{L}^2(\Omega)$  and thus further preconditioning is not necessary.

The new method is introduced and analyzed in detail in the remainder of the paper. In Section 2, we define the weak variational formulation and discuss its solvability and relation to the original problem. Two different discrete least-squares algorithms for the approximation of the proposed weak formulation are considered in Section 3. In both cases, we use different test and solution spaces composed of piecewise polynomial finite elements. We show how the discrete approximation can be stabilized by an appropriate modification of the test space (in Section 3.1) or the bilinear form (in Section 3.2). An optimal order error estimate for solutions with low regularity is proved in Section 3.3. We conclude the paper by discussing the results of some numerical computations in Section 4.

## 2. THE WEAK FORMULATION

In this paper we restrict ourselves to domains  $\Omega$  which are simply connected polyhedrons with Lipschitz continuous and connected boundary. The functions  $\varepsilon$  and  $\mu$  are assumed to be uniformly bounded from above and bounded away from zero. We will also assume that  $\lambda$  is not 0 since, when  $\lambda$  is 0, the problem splits into independent magnetostatic and electrostatic problems which have already been analyzed in [5].

Let  $L^2(\Omega)$  be the space of square-integrable, complex valued functions with inner product  $(u, v) = \int_{\Omega} u \cdot \bar{v}$ . The corresponding vector space is  $\mathbf{L}^2(\Omega) = (L^2(\Omega))^3$ , and for convenience we use the same notation,  $(\cdot, \cdot)$ , for its inner product. Let  $\mathbf{H}^{\gamma}(\Omega)$ ,  $\gamma \in (0, 1]$ , be the Sobolev interpolation space and  $\mathbf{H}^{-\gamma}(\Omega) = \mathbf{H}^{\gamma}(\Omega)^*$  be its dual (see, e.g., [1]). We denote their norms with  $\|\cdot\|_{\gamma}$  and  $\|\cdot\|_{-\gamma}$  respectively. Note that by the dual of a complex Hilbert space  $Y$ , we mean the space  $Y^*$  consisting of all bounded *conjugate-linear* functionals  $\ell$ , i.e.  $\ell(\lambda x + y) = \bar{\lambda} \ell(x) + \ell(y)$  for any  $x, y$  in  $Y$  and  $\lambda \in \mathbb{C}$ .

The vector fields that we are interested in belong to the following spaces (see [20] for more details):

$$\begin{aligned} \mathbf{H}(\mathbf{curl}) &= \{\mathbf{v} \in \mathbf{L}^2(\Omega) : \nabla \times \mathbf{v} \in \mathbf{L}^2(\Omega)\}, \\ \mathbf{H}_0(\mathbf{curl}) &= \{\mathbf{v} \in \mathbf{H}(\mathbf{curl}) : \mathbf{v} \times \mathbf{n} = \mathbf{0} \text{ on } \partial\Omega\}, \\ \mathbf{H}(\text{div}; \varepsilon) &= \{\mathbf{v} \in \mathbf{L}^2(\Omega) : \nabla \cdot (\varepsilon \mathbf{v}) \in L^2(\Omega)\}, \\ \mathbf{H}_0(\text{div}; \mu) &= \{\mathbf{v} \in \mathbf{H}(\text{div}; \mu) : (\mu \mathbf{v}) \cdot \mathbf{n} = 0 \text{ on } \partial\Omega\}, \\ \mathbf{X}_1(\mu) &= \mathbf{H}(\mathbf{curl}) \cap \mathbf{H}_0(\text{div}; \mu), \\ \mathbf{X}_2(\varepsilon) &= \mathbf{H}_0(\mathbf{curl}) \cap \mathbf{H}(\text{div}; \varepsilon). \end{aligned}$$

We will use the same notation to describe the real counterparts of the above spaces.

Consider the problem (1.1). A formal application of the divergence operator leads to the following additional constraints:

$$(2.1) \quad \begin{cases} \nabla \cdot (\mu \mathbf{h}) = \lambda^{-1} \nabla \cdot \mathbf{m} & \text{in } \Omega, \\ \nabla \cdot (\varepsilon \mathbf{e}) = -\lambda^{-1} \nabla \cdot \mathbf{j} & \text{in } \Omega. \end{cases}$$

A standard interpretation of (1.1)-(2.1) is to assume that  $\mathbf{j}$  is in  $\mathbf{H}(\text{div}) \equiv \mathbf{H}(\text{div}; 1)$  and  $\mathbf{m}$  is in  $\mathbf{H}_0(\text{div}) \equiv \mathbf{H}_0(\text{div}; 1)$  and to search for solutions  $\mathbf{h}$  in  $\mathbf{X}_1(\mu)$  and  $\mathbf{e}$  in  $\mathbf{X}_2(\varepsilon)$ . In the remainder of the paper, we refer to this choice as the *original form* of the time-harmonic problem.

The system (1.1)-(2.1) is generally indefinite, i.e. the homogeneous problem with  $\mathbf{j} = \mathbf{m} = \mathbf{0}$  may have nontrivial solutions. In fact, the case  $\mathbf{j} = \mathbf{m} = \mathbf{0}$  is known as the *eigenvalue problem*, where one solves for the eigenvalues  $\lambda \neq 0$  with corresponding nonzero eigenfunctions  $\mathbf{h} \in \mathbf{X}_1(\mu)$ ,  $\mathbf{e} \in \mathbf{X}_2(\varepsilon)$  satisfying

$$(2.2) \quad \begin{cases} \nabla \times \mathbf{h} = \lambda \varepsilon \mathbf{e} & \text{in } \Omega, \\ \nabla \times \mathbf{e} = -\lambda \mu \mathbf{h} & \text{in } \Omega. \end{cases}$$

Problem (2.2) is important on its own, but clearly some knowledge of the eigenvalues is essential for the solvability of the time-harmonic problem. The computation of Maxwell eigenvalues has already been extensively investigated, and there are several stable discretization algorithms, see [9, 11, 20]. One approach that is closely related to the present paper is the least-squares method from [4], which is based on the solution operators for two div-curl systems associated with each of the fields  $\mathbf{h}$  and  $\mathbf{e}$ .

*Remark 2.1.* Usually, in practice,  $\mathbf{m} = \mathbf{0}$ . Then, a popular choice is to reduce the problem to a curl-curl equation for one of the fields. For example, by eliminating the magnetic field, we get

$$(2.3) \quad \nabla \times \mu^{-1} \nabla \times \mathbf{e} = \omega^2 \varepsilon \mathbf{e} + \tilde{\mathbf{j}},$$

where  $\tilde{\mathbf{j}} = -\lambda \mathbf{j}$  and  $\mathbf{e} \times \mathbf{n} = \mathbf{0}$  on the boundary. The weak formulation of (2.3) reads: Find  $\mathbf{e} \in \mathbf{H}_0(\text{curl})$  such that

$$(2.4) \quad (\mu^{-1} \nabla \times \mathbf{e}, \nabla \times \mathbf{w}) = \omega^2 (\varepsilon \mathbf{e}, \mathbf{w}) + (\tilde{\mathbf{j}}, \mathbf{w}) \quad \text{for all } \mathbf{w} \in \mathbf{H}_0(\text{curl}).$$

The case  $\tilde{\mathbf{j}} = \mathbf{0}$  corresponds to the eigenvalue problem.

The solvability of the above weak formulation is characterized by the following result, given as Corollary 4.19 in [20].

**Theorem 2.1.** *Suppose that  $\omega^2 \neq 0$  is not a real Maxwell eigenvalue in the sense that it is not a solution to (2.4) with  $\tilde{\mathbf{j}} = \mathbf{0}$  and nonzero real  $\mathbf{e}$ . Then the curl-curl problem (2.4) has a unique solution  $\mathbf{e}$  for any data  $\tilde{\mathbf{j}} \in \mathbf{L}^2(\Omega)$ , and we have the stability estimate*

$$(2.5) \quad \|\mathbf{e}\|_{\mathbf{H}_0(\text{curl})} \leq C \|\tilde{\mathbf{j}}\|.$$

The next remark shows that in this paper (where  $\varepsilon$  and  $\mu$  are real) we can restrict our attention to a problem involving only real quantities.

*Remark 2.2.* Note that  $(\mathbf{h}, \mathbf{e}, \mathbf{j}, \mathbf{m})$  is a solution to (1.1) with  $\lambda = -i\omega$ ,  $\omega \in \mathbb{R}$  if, and only if,  $(\Re(\mathbf{h}), \Im(\mathbf{e}), \Re(\mathbf{j}), \Im(\mathbf{m}))$  and  $(-\Im(\mathbf{h}), \Re(\mathbf{e}), -\Im(\mathbf{j}), \Re(\mathbf{m}))$  satisfy the related real problem

$$(2.6) \quad \begin{cases} \nabla \times \mathbf{h} = \omega \varepsilon \mathbf{e} + \mathbf{j} & \text{in } \Omega, \\ \nabla \times \mathbf{e} = \omega \mu \mathbf{h} + \mathbf{m} & \text{in } \Omega, \\ \mu \mathbf{h} \cdot \mathbf{n} = 0 & \text{on } \partial\Omega, \\ \mathbf{e} \times \mathbf{n} = \mathbf{0} & \text{on } \partial\Omega, \end{cases}$$

with corresponding divergence equations

$$(2.7) \quad \begin{cases} \nabla \cdot (\mu \mathbf{h}) = -\omega^{-1} \nabla \cdot \mathbf{m} & \text{in } \Omega, \\ \nabla \cdot (\varepsilon \mathbf{e}) = -\omega^{-1} \nabla \cdot \mathbf{j} & \text{in } \Omega. \end{cases}$$

In the implementation, one may prefer to restrict to real fields and consider (2.6)-(2.7) instead of (1.1)-(2.1). This avoids the use of complex arithmetic.

We next proceed to the main task of this section; the introduction of the weak variational formulation. Our motivation is that we have to allow for discontinuous solutions, and in fact, we will only assume that  $\mathbf{h}$  and  $\mathbf{e}$  are in  $\mathbf{L}^2(\Omega)$ . A standard way to relax the regularity requirements  $\mathbf{h} \in \mathbf{X}_1(\mu)$ ,  $\mathbf{e} \in \mathbf{X}_2(\varepsilon)$  is to integrate by parts, choosing test spaces which eliminate the boundary terms. Alternatively, this can be viewed as replacing the differential operators in (1.1)-(2.1) with weaker operators  $\mathbf{curl}_1$ ,  $\mathbf{curl}_2$ ,  $div_{1,\mu}$  and  $div_{2,\varepsilon}$ . These operators map  $\mathbf{L}^2(\Omega)$  into the duals of the following test spaces

$$(2.8) \quad \mathbf{V}_1 = \mathbf{H}_0^1(\Omega), \quad \mathbf{V}_2 = \mathbf{H}^1(\Omega), \quad H_1 = H^1(\Omega), \quad \text{and} \quad H_2 = H_0^1(\Omega).$$

Specifically,  $\mathbf{curl}_1 : \mathbf{L}^2(\Omega) \mapsto \mathbf{V}_1^*$  and  $div_{1,\mu} : \mathbf{L}^2(\Omega) \mapsto H_1^*$  are defined by

$$(2.9) \quad \begin{aligned} \langle \mathbf{curl}_1 \mathbf{h}, \phi \rangle &= (\mathbf{h}, \nabla \times \phi) \quad \text{for all } \mathbf{h} \in \mathbf{L}^2(\Omega), \phi \in \mathbf{V}_1, \\ \langle div_{1,\mu} \mathbf{h}, \psi \rangle &= -(\mu \mathbf{h}, \nabla \psi) \quad \text{for all } \mathbf{h} \in \mathbf{L}^2(\Omega), \psi \in H_1. \end{aligned}$$

Similarly,  $\mathbf{curl}_2 : \mathbf{L}^2(\Omega) \mapsto \mathbf{V}_2^*$  and  $div_{2,\varepsilon} : \mathbf{L}^2(\Omega) \mapsto H_2^*$  satisfy

$$(2.10) \quad \begin{aligned} \langle \mathbf{curl}_2 \mathbf{e}, \phi \rangle &= (\mathbf{e}, \nabla \times \phi) \quad \text{for all } \mathbf{e} \in \mathbf{L}^2(\Omega), \phi \in \mathbf{V}_2, \\ \langle div_{2,\varepsilon} \mathbf{e}, \psi \rangle &= -(\varepsilon \mathbf{e}, \nabla \psi) \quad \text{for all } \mathbf{e} \in \mathbf{L}^2(\Omega), \psi \in H_2. \end{aligned}$$

Given  $\mathbf{j} \in \mathbf{V}_1^*$ ,  $\mathbf{m} \in \mathbf{V}_2^*$ ,  $q \in H_1^*$  and  $\rho \in H_2^*$ , consider the problem of finding  $\mathbf{h}, \mathbf{e} \in \mathbf{L}^2(\Omega)$  such that

$$(2.11) \quad \mathcal{B}_\lambda(\mathbf{h}, \mathbf{e}) \equiv \begin{pmatrix} \mathbf{curl}_1 \mathbf{h} - \lambda \varepsilon \mathbf{e} \\ \mathbf{curl}_2 \mathbf{e} + \lambda \mu \mathbf{h} \\ div_{1,\mu} \mathbf{h} \\ div_{2,\varepsilon} \mathbf{e} \end{pmatrix} = \begin{pmatrix} \mathbf{j} \\ \mathbf{m} \\ q \\ \rho \end{pmatrix}.$$

Set

$$X = \mathbf{L}^2(\Omega) \times \mathbf{L}^2(\Omega) \quad \text{and} \quad Y = \mathbf{V}_1 \times \mathbf{V}_2 \times H_1 \times H_2.$$

Then  $\mathcal{B}_\lambda$  is a bounded linear operator from  $X$  into  $Y^*$ . We say that  $X$  is the *solution* space and  $Y$  is the *test* space.

First, we note that any solution to the original time-harmonic problem satisfies (2.11) with  $q = \lambda^{-1} \nabla \cdot \mathbf{m}$  and  $\rho = -\lambda^{-1} \nabla \cdot \mathbf{j}$ . Indeed, the first equations of (1.1) and (2.1) imply

$$(2.12) \quad \begin{aligned} (\mathbf{h}, \nabla \times \phi) - (\lambda \varepsilon \mathbf{e}, \phi) &= (\mathbf{j}, \phi) \quad \text{for all } \phi \in \mathbf{V}_1, \\ -(\mu \mathbf{h}, \nabla \psi) &= (q, \psi) \quad \text{for all } \psi \in H_1, \end{aligned}$$

where  $q = \lambda^{-1} \nabla \cdot \mathbf{m}$ . These are exactly the first and the third equations in (2.11), and the rest follows similarly.

On the other hand, suppose that  $\mathbf{j}, \mathbf{m} \in \mathbf{L}^2(\Omega)$ ,  $q, \rho \in L^2(\Omega)$  and the pair  $(\mathbf{h}, \mathbf{e}) \in X$  satisfies (2.11). Then (2.12) implies  $\mathbf{h} \in \mathbf{X}_1(\mu)$  and therefore  $(\mathbf{h}, \mathbf{e})$  satisfies the first

equation of the original time-harmonic system. Analogously, we get  $\mathbf{e} \in \mathbf{X}_2(\varepsilon)$ , and therefore  $(\mathbf{h}, \mathbf{e})$  satisfies (1.1). Furthermore, it follows that  $\mathbf{j} \in \mathbf{H}(\text{div})$ ,  $\mathbf{m} \in \mathbf{H}_0(\text{div})$ , and thus  $(\mathbf{h}, \mathbf{e})$  also satisfies (2.1). Note that in this case  $q = \lambda^{-1} \nabla \cdot \mathbf{m}$  and  $\rho = -\lambda^{-1} \nabla \cdot \mathbf{j}$ .

The above considerations imply, in particular,

$$(2.13) \quad \mathcal{B}_\lambda(\mathbf{h}, \mathbf{e}) = 0 \quad \text{if and only if} \quad (\mathbf{h}, \mathbf{e}, \lambda) \quad \text{satisfies} \quad (2.2).$$

It follows that, if  $\lambda$  is not a Maxwell eigenvalue, the kernel of  $\mathcal{B}_\lambda$  is trivial. In fact, a stronger result holds.

**Lemma 2.1.** *Assume that  $\lambda \neq 0$  is not a Maxwell eigenvalue, i.e., it does not satisfy (2.2). Then the operator  $\mathcal{B}_\lambda$  is bounded from below, i.e. there exists a positive constant  $C$  such that*

$$(2.14) \quad \|\mathbf{h}\| + \|\mathbf{e}\| \leq C \|\mathcal{B}_\lambda(\mathbf{h}, \mathbf{e})\|_{Y^*}$$

for all  $(\mathbf{h}, \mathbf{e}) \in X$ .

*Proof.* First, since  $\varepsilon$  and  $\mu$  are piecewise smooth, the operators of multiplication by  $\varepsilon$  and  $\mu$  are bounded from  $\mathbf{H}^\gamma(\Omega)$  to  $\mathbf{H}^\gamma(\Omega)$  for all  $\gamma \in [0, \frac{1}{2})$  (see, e.g., [4]). Second, we recall that, as shown in [5], there exists a constant  $C = C(\mu, \varepsilon) > 0$  such that, for all  $\mathbf{x} \in \mathbf{L}^2(\Omega)$

$$(2.15) \quad C \|\mathbf{x}\|_{\mathbf{L}^2(\Omega)}^2 \leq \|\mathbf{curl}_1 \mathbf{x}\|_{\mathbf{V}_1^*}^2 + \|\text{div}_{1,\mu} \mathbf{x}\|_{H_1^*}^2$$

and

$$(2.16) \quad C \|\mathbf{x}\|_{\mathbf{L}^2(\Omega)}^2 \leq \|\mathbf{curl}_2 \mathbf{x}\|_{\mathbf{V}_2^*}^2 + \|\text{div}_{2,\varepsilon} \mathbf{x}\|_{H_2^*}^2.$$

Here, and in the rest of the paper, we use the symbol  $C$  to denote a generic positive constant which may be different in the different occurrences.

We will prove (2.14) by contradiction, using a standard compactness argument. Now, assume that (2.14) does not hold. Then there exists a sequence  $\{x_n\} = \{(\mathbf{h}_n, \mathbf{e}_n)\} \subset X$  such that  $\|x_n\|^2 \equiv \|\mathbf{h}_n\|^2 + \|\mathbf{e}_n\|^2 = 1$ , while  $\|\mathcal{B}_\lambda x_n\|_{Y^*}^2 \leq \frac{1}{n}$ . Using the fact that  $\mathbf{L}^2(\Omega)$  is compactly embedded in  $\mathbf{H}^{-\gamma}(\Omega)$ , and passing to a subsequence, we get  $\mathbf{h}_n \xrightarrow{H^{-\gamma}} \mathbf{h}$  and  $\mathbf{e}_n \xrightarrow{H^{-\gamma}} \mathbf{e}$  for some  $\mathbf{h}, \mathbf{e} \in \mathbf{H}^{-\gamma}(\Omega)$ . Since  $\gamma < \frac{1}{2}$ , we also have the continuous embeddings  $\|\mathbf{v}\|_{\mathbf{V}_k^*} \leq C \|\mathbf{v}\|_{-\gamma}$  for  $k = 1, 2$ . In particular,  $\mathbf{h} \in \mathbf{V}_1^*$  and  $\mathbf{e} \in \mathbf{V}_2^*$ . Note that the choice of  $\gamma$  implies

$$(2.17) \quad \|\mu \mathbf{h}_n\|_{\mathbf{V}_1^*} \leq C \sup_{\mathbf{w} \in H^\gamma} \frac{|(\mathbf{h}_n, \mu \mathbf{w})|}{\|\mathbf{w}\|_\gamma} \leq C \sup_{\mathbf{v} \in H^\gamma} \frac{|(\mathbf{h}_n, \mathbf{v})|}{\|\mathbf{v}\|_\gamma} = \|\mathbf{h}_n\|_{-\gamma}$$

for any  $\mathbf{h}_n \in \mathbf{L}^2(\Omega)$ . By (2.15) and (2.16),

$$\|x_n\|^2 \leq C \left\{ \|\mathbf{curl}_1 \mathbf{h}_n\|_{\mathbf{V}_1^*}^2 + \|\text{div}_{1,\mu} \mathbf{h}_n\|_{H_1^*}^2 + \|\mathbf{curl}_2 \mathbf{e}_n\|_{\mathbf{V}_2^*}^2 + \|\text{div}_{2,\varepsilon} \mathbf{e}_n\|_{H_2^*}^2 \right\}.$$

Therefore, for  $m, n \in \mathbb{N}$ ,

$$\|x_m - x_n\|^2 \leq C \left\{ \|\mathcal{B}_\lambda(x_m - x_n)\|_{Y^*}^2 + \omega^2 \|\mu \mathbf{h}_m - \mu \mathbf{h}_n\|_{\mathbf{V}_1^*}^2 + \omega^2 \|\varepsilon \mathbf{e}_m - \varepsilon \mathbf{e}_n\|_{\mathbf{V}_2^*}^2 \right\}.$$

Using (2.17) and the above inequality, we get that  $\{x_n\}$  is a Cauchy sequence in  $X$ .

Therefore, we can conclude that  $x = (\mathbf{h}, \mathbf{e}) \in X$  and  $x_n \xrightarrow{X} x$ .

After passing to a limit, we get  $\|x\| = 1$ , while  $\mathcal{B}_\lambda x = 0$ . Since  $\lambda$  is not an eigenvalue, (2.13) implies  $x = 0$ , which is a contradiction.  $\square$

*Remark 2.3.* The terms involving  $div_{1,\mu}$  and  $div_{2,\varepsilon}$  cannot be omitted from the right hand side of (2.14). For example, that the  $div_{2,\varepsilon}$  term is necessary can easily be seen by taking  $\mathbf{h} = 0$  and  $\mathbf{e} = \nabla\phi$  with  $\phi \in C_0^\infty(\Omega)$ .

The fact that  $\mathcal{B}_\lambda$  satisfies (2.14) implies that its range is closed and therefore, (2.11) has a unique solution if and only if the right-hand side is in the range of  $\mathcal{B}_\lambda$ . Our next task is to characterize this subspace. We first note that the range of  $\mathcal{B}_\lambda$  coincides with

$$(Ker(\mathcal{B}_\lambda^*))^\perp = \{y^* \in Y^* : \langle y^*, y \rangle = 0 \text{ for all } y \in Ker(\mathcal{B}_\lambda^*)\}.$$

Here

$$Ker(\mathcal{B}_\lambda^*) = \{(\mathbf{v}_1, \mathbf{v}_2, h_1, h_2) \in Y : b_\lambda(\mathbf{h}, \mathbf{e}; \mathbf{v}_1, \mathbf{v}_2, h_1, h_2) = 0 \text{ for all } (\mathbf{h}, \mathbf{e}) \in X\}$$

and  $b_\lambda(\cdot, \cdot)$  is the bilinear form corresponding to  $\mathcal{B}_\lambda$ , i.e.,

$$(2.18) \quad \begin{aligned} b_\lambda(\mathbf{h}, \mathbf{e}; \mathbf{v}_1, \mathbf{v}_2, h_1, h_2) &= b_1(\mathbf{h}; \mathbf{v}_1, h_1) - \lambda(\varepsilon\mathbf{e}, \mathbf{v}_1) \\ &\quad + b_2(\mathbf{e}; \mathbf{v}_2, h_2) + \lambda(\mu\mathbf{h}, \mathbf{v}_2) \end{aligned}$$

where the forms  $b_k(\cdot, \cdot)$  are given by

$$b_1(\mathbf{h}; (\mathbf{v}_1, h_1)) = (\mathbf{h}, \nabla \times \mathbf{v}_1) - (\mu\mathbf{h}, \nabla h_1) \text{ and } b_2(\mathbf{e}; (\mathbf{v}_2, h_2)) = (\mathbf{e}, \nabla \times \mathbf{v}_2) - (\varepsilon\mathbf{e}, \nabla h_2).$$

Now, if  $(\mathbf{v}_1, \mathbf{v}_2, h_1, h_2)$  is in  $Ker(\mathcal{B}_\lambda^*)$  then

$$\begin{cases} \nabla \times \mathbf{v}_1 + \lambda\mu\mathbf{v}_2 - \mu\nabla h_1 = 0, \\ \nabla \times \mathbf{v}_2 - \lambda\varepsilon\mathbf{v}_1 - \varepsilon\nabla h_2 = 0. \end{cases}$$

Set  $\tilde{\mathbf{v}}_1 = \mathbf{v}_1 + \lambda^{-1}\nabla h_2$  and  $\tilde{\mathbf{v}}_2 = \mathbf{v}_2 - \lambda^{-1}\nabla h_1$ . It follows that  $\tilde{\mathbf{v}}_1 \in \mathbf{X}_2(\varepsilon)$  and  $\tilde{\mathbf{v}}_2 \in \mathbf{X}_1(\mu)$  satisfy the eigenvalue problem (2.2). This implies, assuming that  $\lambda$  is not an eigenvalue,

$$(2.19) \quad \mathbf{v}_1 = -\lambda^{-1}\nabla h_2 \quad \text{and} \quad \mathbf{v}_2 = \lambda^{-1}\nabla h_1.$$

Conversely, if (2.19) holds with  $(\mathbf{v}_1, \mathbf{v}_2, h_1, h_2) \in Y$ , then clearly  $(\mathbf{v}_1, \mathbf{v}_2, h_1, h_2)$  is in  $Ker(\mathcal{B}_\lambda^*)$ . The next result follows easily.

**Lemma 2.2.** *Assume that  $\lambda$  is not a Maxwell eigenvalue. Then the compatibility space for (2.11) is given by*

$$(2.20) \quad \mathbf{V}_{\lambda,0} \equiv Ker(\mathcal{B}_\lambda^*) = \{(-\nabla h_2, \nabla h_1, \lambda h_1, \lambda h_2) : h_1 \in H^2(\Omega), h_2 \in H_0^2(\Omega)\}.$$

Consequently, the data  $(\mathbf{j}, \mathbf{m}, q, \rho)$  are compatible if, and only if,

$$(2.21) \quad \langle \rho, h_2 \rangle = \lambda^{-1} \langle \mathbf{j}, \nabla h_2 \rangle, \quad \langle q, h_1 \rangle = -\lambda^{-1} \langle \mathbf{m}, \nabla h_1 \rangle,$$

for all  $h_2 \in H_0^2(\Omega)$ ,  $h_1 \in H^2(\Omega)$ . When  $\mathbf{j}$  is in  $\mathbf{H}(\text{div})$  and  $\mathbf{m}$  is in  $\mathbf{H}_0(\text{div})$ , the above conditions simplify to

$$(2.22) \quad \rho = -\lambda^{-1}\nabla \cdot \mathbf{j}, \quad q = \lambda^{-1}\nabla \cdot \mathbf{m}.$$

We combine the results of Lemma 2.1 and Lemma 2.2 in the main result of this section.

**Theorem 2.2.** *Assume that  $\lambda \neq 0$  is not a Maxwell eigenvalue. Then the weak formulation (2.11) has a unique solution for any data satisfying the compatibility conditions (2.21). The following stability estimate holds*

$$C(\|\mathbf{h}\| + \|\mathbf{e}\|) \leq \|\mathbf{j}\|_{\mathbf{V}_1^*} + \|\mathbf{m}\|_{\mathbf{V}_2^*} + \|q\|_{H_1^*} + \|\rho\|_{H_2^*}.$$

When  $\mathbf{j} \in \mathbf{H}(\text{div})$ ,  $\mathbf{m} \in \mathbf{H}_0(\text{div})$  and  $\rho$  and  $q$  are defined by (2.22), the weak solution coincides with the solution of the original time-harmonic problem (1.1), and we have

$$(2.23) \quad C (\|\mathbf{h}\|_{\mathbf{X}_1(\mu)} + \|\mathbf{e}\|_{\mathbf{X}_2(\varepsilon)}) \leq \|\mathbf{j}\|_{\mathbf{H}(\text{div})} + \|\mathbf{m}\|_{\mathbf{H}(\text{div})}.$$

Note that Theorem 2.1 is a special case of the above result.

*Proof.* The first estimate is identical to the result of Lemma 2.1.

If  $\mathbf{j} \in \mathbf{H}(\text{div})$ ,  $\mathbf{m} \in \mathbf{H}_0(\text{div})$  and  $\rho$  and  $q$  are defined by (2.22), then  $\rho$  and  $q$  are in  $L^2(\Omega)$ , and earlier arguments show that the weak formulation has a unique solution which satisfies the original time-harmonic problem (1.1)-(2.1). The first part of the theorem shows that

$$C (\|\mathbf{h}\| + \|\mathbf{e}\|) \leq \|\mathbf{j}\|_{\mathbf{H}(\text{div})} + \|\mathbf{m}\|_{\mathbf{H}(\text{div})}.$$

The bounds for the remaining terms in (2.23) follow from this, (1.1), (2.1) and the triangle inequality.  $\square$

*Remark 2.4.* The weak form of the real problem (2.6)-(2.7) is based on the operator

$$(2.24) \quad \mathcal{B}_\omega(\mathbf{h}, \mathbf{e}) = (\mathbf{curl}_1 \mathbf{h} - \omega \varepsilon \mathbf{e}, \mathbf{curl}_2 \mathbf{e} - \omega \mu \mathbf{h}, \text{div}_{1,\mu} \mathbf{h}, \text{div}_{2,\varepsilon} \mathbf{e}),$$

where all fields, spaces and operators are real. The corresponding bilinear form is given by

$$b_\omega(\cdot, \cdot) = b_1(\mathbf{h}; \mathbf{v}_1, h_1) - \omega(\varepsilon \mathbf{e}, \mathbf{v}_1) + b_2(\mathbf{e}; \mathbf{v}_2, h_2) - \omega(\mu \mathbf{h}, \mathbf{v}_2).$$

The compatibility space in this case is

$$(2.25) \quad \mathbf{V}_{\omega,0} \equiv \text{Ker}(\mathcal{B}_\omega^*) = \{(\nabla h_2, \nabla h_1, \omega h_1, \omega h_2) : h_1 \in H^2(\Omega), h_2 \in H_0^2(\Omega)\}.$$

### 3. LEAST-SQUARES APPROXIMATION

Next we consider the discrete approximation to the weak variational formulation presented in Section 2. We assume that  $\lambda = -i\omega$  is not a Maxwell eigenvalue and that the domain  $\Omega$  is a polyhedron (or a polygon in 2D) that is partitioned in a shape regular and locally quasi-uniform mesh  $\mathbb{T}_h = \{T\}$ . The diameter of an element  $T \in \mathbb{T}_h$  is denoted with  $h_T$ . We assume that the coefficients  $\varepsilon$  and  $\mu$  are constants on each element  $T$ . We also concentrate on the case of real fields, i.e. we approximate (2.6)-(2.7).

Let  $f = (\mathbf{j}, \mathbf{m}, q, \rho) \in Y^*$ . Then the problem (2.6)-(2.7) can be rewritten (see Remark 2.4) equivalently as follows: Find  $(\mathbf{h}, \mathbf{e}) \in X$  such that

$$(3.1) \quad b_\omega(\mathbf{h}, \mathbf{e}; \mathbf{v}_1, \mathbf{v}_2, h_1, h_2) = \langle f; \mathbf{v}_1, \mathbf{v}_2, h_1, h_2 \rangle \quad \text{for all } (\mathbf{v}_1, \mathbf{v}_2, h_1, h_2) \in Y.$$

In what follows, we discuss two methods for the discrete approximation of (3.1). The first requires a discrete inf-sup condition, while the second is based on form modification.

Let  $X_h = X_{h,1} \times X_{h,2} \subseteq X$  and  $Y_h = \mathbf{V}_{h,1} \times \mathbf{V}_{h,2} \times H_{h,1} \times H_{h,2} \subseteq Y$  be piecewise polynomial finite element spaces defined on  $\mathbb{T}_h$ . One simple choice is  $X_{h,1} = X_{h,2} = (\widehat{S}_h)^3$  and  $Y_h = (S_{h,0})^3 \times (S_h)^3 \times S_h \times S_{h,0}$ , where  $\widehat{S}_h$  is a discontinuous solution space, while  $S_h$  and  $S_{h,0} = S_h \cap H_0^1(\Omega)$  are continuous test spaces. Approximation with spaces of varying polynomial degree is also possible. We assume the existence of a stable approximation operator  $\mathcal{I}_h$ , such that  $\mathcal{I}_h : H^1(\Omega) \mapsto S_h$ ,  $\mathcal{I}_h : H_0^1(\Omega) \mapsto S_{h,0}$  and

$$(3.2) \quad \sum_{T \in \mathbb{T}_h} \left\{ h_T^{-2} \|u - \mathcal{I}_h u\|_{L^2(T)}^2 + \|\mathcal{I}_h u\|_{H^1(T)}^2 \right\} \leq C \|u\|_{H^1(\Omega)}^2.$$

Such operators are known to exist when  $S_h$  is the space of standard Lagrangian finite elements, see [6, 25].

**3.1. Approximation based on a discrete inf-sup condition.** In this subsection, we are interested in pairs of approximation spaces  $(X_h, Y_h)$  satisfying the discrete inf-sup condition,

$$(3.3) \quad \|x\|_X \leq C \sup_{y \in Y_h} \frac{b_\omega(x; y)}{\|y\|_Y}, \quad \text{for all } x \in X_h,$$

with a constant  $C > 0$  independent of  $h$ . The condition (3.3) is equivalent to the condition that the discrete analog of  $\mathcal{B}_\omega$ , the operator  $\mathcal{B}_{h,\omega} : X_h \rightarrow Y_h^*$ , defined by

$$\langle \mathcal{B}_{h,\omega} x, y \rangle = b_\omega(x, y), \quad \text{for all } x \in X_h, y \in Y_h,$$

has a uniformly (independent of  $h$ ) bounded inverse on its range.

Assuming (3.3), one can consider an approximation to (3.1) obtained by restricting the form to the discrete subspaces. The resulting problem is  $\mathcal{B}_{h,\omega}(\mathbf{h}_h, \mathbf{e}_h) = f_h$  where  $f_h$  is the restriction of  $f$  to  $Y_h^*$ . Unfortunately, even though  $\mathcal{B}_{h,\omega}$  is invertible on its range, this problem is not likely to be solvable since the discrete compatibility of  $f_h$  does not follow from the compatibility of  $f$ .

A natural way to avoid this obstacle is to consider a least-squares approximation, which always has a unique solution, regardless of the data. Specifically, the least-squares approximate solution  $(\mathbf{h}_h, \mathbf{e}_h) = x_h$  is the unique element of  $X_h$  satisfying

$$(3.4) \quad \langle \mathcal{B}_{h,\omega} x_h, \mathcal{T}_{Y_h} \mathcal{B}_{h,\omega} \tilde{x}_h \rangle = \langle f, \mathcal{T}_{Y_h} \mathcal{B}_{h,\omega} \tilde{x}_h \rangle, \quad \text{for all } \tilde{x}_h \in X_h,$$

where  $\mathcal{T}_{Y_h} : Y_h^* \rightarrow Y_h$  is the solution operator defined by

$$(\mathcal{T}_{Y_h} l, y_h)_Y = \langle l, y_h \rangle \quad \text{for all } y_h \in Y_h.$$

As discussed in [5], the problem (3.4) reduces to inverting a symmetric and positive definite matrix which is spectrally equivalent to the mass matrix in  $X$ . The resulting approximation is quasi-optimal, i.e. if  $x \in X$  satisfies  $\mathcal{B}_\omega x = f$ , then there exists  $C = C(\varepsilon, \mu, \omega)$  independent of  $h$ , such that

$$(3.5) \quad \|x - x_h\|_X \leq C \inf_{\xi_h \in X_h} \|x - \xi_h\|_X,$$

where  $x_h$  is the solution of (3.4). In the implementation, one can replace  $\mathcal{T}_{Y_h}$  by a preconditioner  $\tilde{\mathcal{T}}_{Y_h} : Y_h^* \rightarrow Y_h$ , preserving the above properties.

*Remark 3.1.* We note that  $\tilde{\mathcal{T}}_{Y_h}$  and  $\mathcal{T}_{Y_h}$  provide representations of the inner product on  $Y_h^*$ , i.e.,

$$(x, y)_{Y_h^*} = \langle x, \tilde{\mathcal{T}}_{Y_h} y \rangle$$

or

$$(x, y)_{Y_h^*} = \langle x, \mathcal{T}_{Y_h} y \rangle.$$

These, in turn, define inner products on the component subspaces which we shall denote by  $(\cdot, \cdot)_{\mathbf{V}_{h,1}^*}$ ,  $(\cdot, \cdot)_{\mathbf{V}_{h,2}^*}$ ,  $(\cdot, \cdot)_{H_{h,1}^*}$  and  $(\cdot, \cdot)_{H_{h,2}^*}$ .

The remainder of this subsection is devoted to the construction of subspaces  $X_h$  and  $Y_h$  satisfying (3.3). For simplicity, we assume that  $\mathbb{T}_h$  is a tetrahedral or triangular partitioning of  $\Omega$ . The extension to quadrilateral and hexahedral meshes is routine.

Let  $\mathcal{P}_p(T)$  be the space of polynomials on  $T$  of degree  $p \in \mathbb{N}_0$ . We will use the following standard finite element spaces

$$\begin{aligned}\widehat{S}_h(p) &= \{v_h \in L^2(\Omega) : v_h|_T \in \mathcal{P}_p(T), \quad \text{for all } T \in \mathbb{T}_h\}, \\ S_h(p) &= \widehat{S}_h(p) \cap H^1(\Omega), \quad S_{h,0}(p) = S_h(p) \cap H_0^1(\Omega).\end{aligned}$$

Additionally, we need spaces of ‘‘bubble’’ functions associated with the faces and the elements, which we introduce below.

Let  $\mathbb{F}_h$  be the set of all faces of  $\mathbb{T}_h$ . Fix  $F \in \mathbb{F}_h$ , and let  $\mathbb{T}_F$  be the union of the elements  $T \in \mathbb{T}_h$  which have  $F$  as a face. Let  $h_F$  be the diameter of  $F$ . Let  $\mathcal{P}_p(F)$  be the space of polynomials of degree  $p$  on a fixed face  $F$ . Let  $d_p$  be the dimension of this space and  $\{\rho_F^j\}_{j=1}^{d_p}$  be the usual nodal basis. Each function  $\rho_F \in \mathcal{P}_p(F)$  can be extended to a polynomial  $\hat{\rho}_F$  of degree  $p$  on  $\mathbb{R}^3$  by setting it to be constant in the direction normal to  $F$ . The basis for the face-bubble function space is defined by

$$(3.6) \quad \beta_F^j|_T(x) = \hat{\rho}_F^j(x) \prod_{i=1}^{N_F} \ell_i(x) \quad \text{for all } T \in \mathbb{T}_F,$$

for each  $1 \leq j \leq d_p$ . Here,  $N_F$  is the number of vertices of  $F$  and  $\{\ell_i(x)\}_{i=1}^{N_F}$  are the barycentric coordinates for  $x \in T$  corresponding to those vertices. Note that  $\beta_F^j$  vanishes on all other faces in  $\mathbb{F}_h$ . The linear span of all these functions forms the space  $B_{\mathbb{F}_h}^p$ . The space  $B_{\mathbb{F}_h,0}^p$  is defined, similarly, using only the interior faces.

A typical element of  $B_{\mathbb{F}_h}^0$  on a triangular mesh and the bubbles for each face of a tetrahedron are shown in Figure 1.

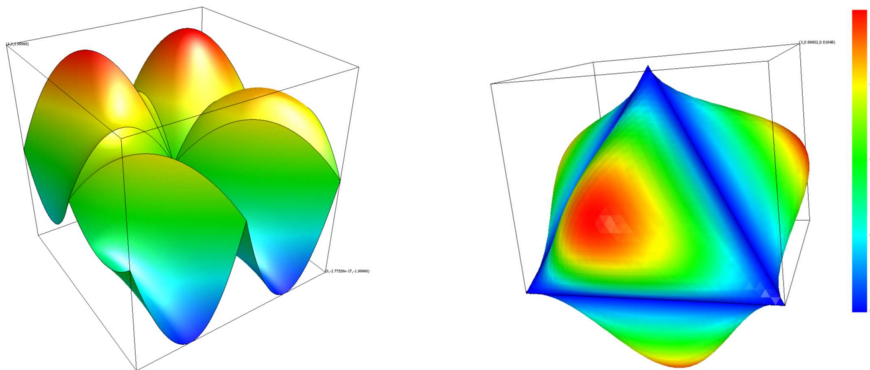


FIGURE 1. Face bubble functions: element of  $B_{\mathbb{F}_h}^0$  in 2D and the bubbles for each face of a tetrahedron in 3D.

The spaces  $B_{\mathbb{T}_h}^p$  of bubble functions of order  $p$  associated with the elements can be defined similarly to (3.6). In fact, the same formula can be used to define the basis element-bubble functions, if the product is taken over the barycentric coordinates corresponding to all vertices of  $T$  and  $\hat{\rho}_F^j$  is replaced by a polynomial  $\rho_T^j \in \mathcal{P}_p(T)$ . Note that  $\beta_T^j$  vanishes on all other elements (by definition). For  $p < 0$ ,  $B_{\mathbb{T}_h}^p$  is defined to be empty.

The next result shows how one can use the face and element bubble functions in order to obtain a stable approximation pair of spaces of fixed polynomial degree  $p$ .

**Theorem 3.1.** *Let  $p$  be in  $\mathbb{N}_0$ . Then the least-squares method (3.4) for the time-harmonic problem based on the spaces  $X_{h,1} = X_{h,2} = (\widehat{S}_h(p))^3$  and*

$$\begin{aligned} \mathbf{V}_{h,1} &= (S_{h,0}(1) \oplus B_{\mathbb{F}_h,0}^p \oplus B_{\mathbb{T}_h}^p)^3, & H_{h,1} &= S_h(1) \oplus B_{\mathbb{F}_h}^p \oplus B_{\mathbb{T}_h}^{p-1}, \\ \mathbf{V}_{h,2} &= (S_h(1) \oplus B_{\mathbb{F}_h}^p \oplus B_{\mathbb{T}_h}^p)^3, & H_{h,2} &= S_{h,0}(1) \oplus B_{\mathbb{F}_h,0}^p \oplus B_{\mathbb{T}_h}^{p-1} \end{aligned}$$

is stable, i.e., the discrete inf-sup condition for the form  $b_\omega(\cdot, \cdot)$  holds.

In particular, the discrete problem (3.4) has a unique solution for any data  $f$ . The resulting approximation is quasi-optimal (in the sense of estimate (3.5)).

*Proof.* Fix  $x = (\mathbf{x}_1, \mathbf{x}_2) \in X_h$ ,  $\psi_k \in H_k$ , and  $\mathbf{v}_k \in \mathbf{V}_k$  for  $k \in \{1, 2\}$ . First, we note that, by a straightforward extension of the proofs of Lemmas 6.3 and 6.4 in [5], we can choose  $\psi_{h,k} \in H_{h,k}$  such that  $(\mu \mathbf{x}_1, \nabla \psi_1) = (\mu \mathbf{x}_1, \nabla \psi_{h,1})$  and  $(\varepsilon \mathbf{x}_2, \nabla \psi_2) = (\varepsilon \mathbf{x}_2, \nabla \psi_{h,2})$  with  $\|\psi_{h,k}\|_1 \leq C \|\psi_k\|_1$ , where  $C > 0$  is independent of  $h$ . In order to satisfy the equalities, the construction uses the stable approximation operator with face and element bubble functions. For the time-harmonic problem, we additionally need to construct  $\mathbf{v}_{h,k} \in \mathbf{V}_{h,k}$  satisfying

$$(3.7) \quad (\mathbf{x}_1, \nabla \times \mathbf{v}_1) - \omega (\varepsilon \mathbf{x}_2, \mathbf{v}_1) = (\mathbf{x}_1, \nabla \times \mathbf{v}_{h,1}) - \omega (\varepsilon \mathbf{x}_2, \mathbf{v}_{h,1})$$

and

$$(3.8) \quad (\mathbf{x}_2, \nabla \times \mathbf{v}_2) - \omega (\mu \mathbf{x}_1, \mathbf{v}_2) = (\mathbf{x}_2, \nabla \times \mathbf{v}_{h,2}) - \omega (\varepsilon \mathbf{x}_1, \mathbf{v}_{h,2})$$

with

$$\|\mathbf{v}_{k,h}\|_1 \leq C \|\mathbf{v}_k\|_1, \quad k = 1, 2.$$

The discrete inf-sup condition then follows from the above constructions and (2.14).

We illustrate the constructions in the case of (3.7). The case of (3.8) is similar. Let  $\mathbf{v}_1 = (v^c)_{c=1}^3$  and  $\mathbf{v}_{h,1} = (v_h^c)_{c=1}^3$ . Set  $v_h^c = \mathcal{I}_h v^c + v_{\mathbb{F}_h}^c + v_{\mathbb{T}_h}^c$ , where  $\mathcal{I}_h$  is an approximation operator satisfying (3.2) and

$$(3.9) \quad \begin{aligned} (v_{\mathbb{F}_h}^c, q)_{L^2(F)} &= (v^c - \mathcal{I}_h v^c, q)_{L^2(F)} && \text{for all } F \in \mathbb{F}_h, q \in \mathcal{P}_p(F), \\ (v_{\mathbb{T}_h}^c, p)_{L^2(T)} &= (v^c - \mathcal{I}_h v^c - v_{\mathbb{F}_h}^c, p)_{L^2(T)} && \text{for all } T \in \mathbb{T}_h, p \in \mathcal{P}_p(T). \end{aligned}$$

Note that (3.9) uniquely determines  $v_{\mathbb{F}_h}^c$  and  $v_{\mathbb{T}_h}^c$ . For example, if  $q \in \mathcal{P}_p(F)$  with  $q \neq 0$ , let  $\hat{q} = \beta_F^j$  where  $\beta_F^j$  is defined by (3.6) with  $\hat{\rho}_F^j$  replaced by  $q$ . Then

$$(\hat{q}, q)_{L^2(F)} = \int_F \left( \prod_{i=1}^{N_F} \ell_i \right) q^2 dx$$

and the unique solvability easily follows.

The definitions in (3.9) imply that

$$\begin{aligned} (\nabla \times \mathbf{x}_1 - \omega \varepsilon \mathbf{x}_2, \mathbf{v}_1)_{L^2(T)} &= (\nabla \times \mathbf{x}_1 - \omega \varepsilon \mathbf{x}_2, \mathbf{v}_{h,1})_{L^2(T)} && \text{for all } T \in \mathbb{T}_h, \\ (\mathbf{x}_1 \times \mathbf{n}, \mathbf{v}_1)_{L^2(F)} &= (\mathbf{x}_1 \times \mathbf{n}, \mathbf{v}_{h,1})_{L^2(F)} && \text{for all } F \in \mathbb{F}_h, \end{aligned}$$

and therefore (3.7) follows. The rest of the proof proceeds as in [5].  $\square$

*Remark 3.2.* Note that, compared to the stable approximation pairs from Section 6 in [5], our theory requires vector test spaces having one degree higher element bubbles. However, the numerical experiments in Section 4 seem to suggest that this is not really necessary.

**3.2. Approximation based on form modification.** Next we consider the least-squares approach based on form modification as presented at the end of Section 6 in [5]. This approach leads to a stable approximation, even when the discrete inf-sup condition does not hold. The idea is to start with the lower bound for  $\mathcal{B}_\omega$ ,

$$(3.10) \quad \|\mathbf{h}\|^2 + \|\mathbf{e}\|^2 \leq C \|\mathcal{B}_\omega(\mathbf{h}, \mathbf{e})\|_{Y^*}^2$$

and use integration by parts on the elements and approximation to get a stable discrete form.

We only consider the case when each component of  $X_h$  is piecewise constant while the components of  $\mathbf{V}_{h,k}$  and  $H_{h,k}$  are continuous piecewise linear functions satisfying the appropriate boundary conditions.

Let  $div_{1,\mu}^h : X_{h,1} \mapsto H_{h,1}$  and  $\mathbf{curl}_{1,\omega}^h : X_{h,1} \times X_{h,2} \mapsto \mathbf{V}_{h,1}$  satisfy

$$\begin{aligned} (div_{1,\mu}^h \mathbf{x}_h, \psi_h) &= -(\mu \mathbf{x}_h, \nabla \psi_h) && \text{for all } \psi_h \in H_{h,1}, \\ (\mathbf{curl}_{1,\omega}^h(\mathbf{x}_{h,1}, \mathbf{x}_{h,2}), \mathbf{w}_h) &= (\mathbf{x}_{h,1}, \nabla \times \mathbf{w}_h) - \omega(\varepsilon \mathbf{x}_{h,2}, \mathbf{w}_h) && \text{for all } \mathbf{w}_h \in \mathbf{V}_{h,1}. \end{aligned}$$

These operators are well defined by the Riesz Representation Theorem, and their computation can be reduced to simple vector operations and the inversion of the mass matrices in  $H_{h,1}$  and  $\mathbf{V}_{h,1}$ . However, the mass matrix inversions are avoided in the actual implementation, because of the way that the preconditioner is defined. One introduces the discrete operators  $div_{2,\varepsilon}^h : X_{h,2} \mapsto H_{h,2}$  and  $\mathbf{curl}_{2,\omega}^h : X_{h,1} \times X_{h,2} \mapsto \mathbf{V}_{h,2}$  in a similar manner,

$$\begin{aligned} (div_{2,\varepsilon}^h \mathbf{x}_h, \psi_h) &= -(\varepsilon \mathbf{x}_h, \nabla \psi_h) && \text{for all } \psi_h \in H_{h,2}, \\ (\mathbf{curl}_{2,\omega}^h(\mathbf{x}_{h,1}, \mathbf{x}_{h,2}), \mathbf{w}_h) &= (\mathbf{x}_{h,2}, \nabla \times \mathbf{w}_h) - \omega(\mu \mathbf{x}_{h,1}, \mathbf{w}_h) && \text{for all } \mathbf{w}_h \in \mathbf{V}_{h,2}. \end{aligned}$$

The following inequalities hold for any  $(\mathbf{h}_h, \mathbf{e}_h) \in X_h$  and result from integration by parts on the elements and (3.2):

$$(3.11) \quad \begin{aligned} C \|div_{1,\mu}^h \mathbf{h}_h\|_{H_1^*}^2 &\leq \|div_{1,\mu}^h \mathbf{h}_h\|_{H_{h,1}^*}^2 + \sum_{F \in \mathbb{F}_h} h_F \|\llbracket \mu \mathbf{h}_h \cdot \mathbf{n} \rrbracket\|_{L^2(F)}^2, \\ C \|\mathbf{curl}_{1,\omega}^h \mathbf{h}_h - \omega \varepsilon \mathbf{e}_h\|_{\mathbf{V}_1^*}^2 &\leq \|\mathbf{curl}_{1,\omega}^h(\mathbf{h}_h, \mathbf{e}_h)\|_{\mathbf{V}_{h,1}^*}^2 \\ &\quad + \sum_{F \in \mathbb{F}_h} h_F \|\llbracket \mathbf{h}_h \times \mathbf{n} \rrbracket\|_{L^2(F)}^2 + \omega^2 \sum_{T \in \mathbb{T}_h} h_T^2 \|\varepsilon \mathbf{e}_h\|_{L^2(T)}^2, \\ C \|div_{2,\varepsilon}^h \mathbf{e}_h\|_{H_2^*}^2 &\leq \|div_{2,\varepsilon}^h \mathbf{e}_h\|_{H_{h,2}^*}^2 + \sum_{F \in \mathbb{F}_h} h_F \|\llbracket \varepsilon \mathbf{e}_h \cdot \mathbf{n} \rrbracket\|_{L^2(F)}^2, \\ C \|\mathbf{curl}_{2,\omega}^h \mathbf{e}_h - \omega \mu \mathbf{h}_h\|_{\mathbf{V}_2^*}^2 &\leq \|\mathbf{curl}_{2,\omega}^h(\mathbf{h}_h, \mathbf{e}_h)\|_{\mathbf{V}_{h,2}^*}^2 \\ &\quad + \sum_{F \in \mathbb{F}_h} h_F \|\llbracket \mathbf{e}_h \times \mathbf{n} \rrbracket\|_{L^2(F)}^2 + \omega^2 \sum_{T \in \mathbb{T}_h} h_T^2 \|\mu \mathbf{h}_h\|_{L^2(T)}^2. \end{aligned}$$

Here  $\llbracket \cdot \rrbracket$  denotes the jump across  $F \in \mathbb{F}_h$ . Inequalities of these types were discussed in detail in [5]. For example, integration by parts, using the fact that  $\nabla \cdot \mathbf{h}_h = 0$  in each element, and the boundedness of  $\mathcal{I}_h$  give

$$\|div_{1,\mu}^h \mathbf{h}_h\|_{H_1^*} \leq C \|div_{1,\mu}^h \mathbf{h}_h\|_{H_{h,1}^*} + \sup_{\phi \in H_1} \frac{\sum_{T \in \mathbb{T}_h} (\mu \mathbf{h}_h \cdot \mathbf{n}, \phi - \mathcal{I}_h \phi)_{L^2(\partial T)}}{\|\phi\|_{H_1}}$$

The first inequality of (3.11) easily follows from this and (3.2). Similarly, we get

$$\begin{aligned} \|\mathbf{curl}_1 \mathbf{h}_h - \omega \varepsilon \mathbf{e}_h\|_{\mathbf{V}_1^*} &\leq C \|\mathbf{curl}_{1,\omega}^h(\mathbf{h}_h, \mathbf{e}_h)\|_{\mathbf{V}_{h,1}^*} \\ &\quad + \sup_{\phi \in \mathbf{V}_1} \frac{\sum_{T \in \mathbb{T}_h} (\mathbf{h}_h \times \mathbf{n}, \phi - \mathcal{I}_h \phi)_{\partial T}}{\|\phi\|_{\mathbf{V}_1}} + \sup_{\phi \in \mathbf{V}_1} \frac{(\omega \varepsilon \mathbf{e}_h, \phi - \mathcal{I}_h \phi)}{\|\phi\|_{\mathbf{V}_1}}, \end{aligned}$$

which implies the second inequality of (3.11).

We then get the least-squares problem: Find  $(\mathbf{h}, \mathbf{e}) \in X_h$  satisfying

$$(3.12) \quad \begin{aligned} b_{h,\omega}(\mathbf{h}, \mathbf{e}; \tilde{\mathbf{h}}, \tilde{\mathbf{e}}) &= (\mathbf{j}, \mathbf{curl}_{1,\omega}^h(\tilde{\mathbf{h}}, \tilde{\mathbf{e}}))_{\mathbf{V}_{h,1}^*} + (\mathbf{m}, \mathbf{curl}_{2,\omega}^h(\tilde{\mathbf{h}}, \tilde{\mathbf{e}}))_{\mathbf{V}_{h,2}^*} \\ &\quad + (q, \operatorname{div}_{1,\mu}^h \tilde{\mathbf{h}})_{H_{h,1}^*} + (\rho, \operatorname{div}_{2,\varepsilon}^h \tilde{\mathbf{e}})_{H_{h,2}^*} \quad \text{for all } (\tilde{\mathbf{h}}, \tilde{\mathbf{e}}) \in X_h. \end{aligned}$$

The bilinear form on the left is given by

$$\begin{aligned} b_{h,\omega}(\mathbf{h}, \mathbf{e}; \tilde{\mathbf{h}}, \tilde{\mathbf{e}}) &= (\mathbf{curl}_{1,\omega}^h(\mathbf{h}, \mathbf{e}), \mathbf{curl}_{1,\omega}^h(\tilde{\mathbf{h}}, \tilde{\mathbf{e}}))_{\mathbf{V}_{h,1}^*} + (\operatorname{div}_{1,\mu}^h \mathbf{h}, \operatorname{div}_{1,\mu}^h \tilde{\mathbf{h}})_{H_{h,1}^*} \\ &\quad + (\mathbf{curl}_{2,\omega}^h(\mathbf{h}, \mathbf{e}), \mathbf{curl}_{2,\omega}^h(\tilde{\mathbf{h}}, \tilde{\mathbf{e}}))_{\mathbf{V}_{h,2}^*} + (\operatorname{div}_{2,\varepsilon}^h \mathbf{e}, \operatorname{div}_{2,\varepsilon}^h \tilde{\mathbf{e}})_{H_{h,2}^*} \\ &\quad + \omega^2 \sum_{T \in \mathbb{T}_h} h_T^2 \{ (\mu \mathbf{h}, \mu \tilde{\mathbf{h}})_{L^2(T)} + (\varepsilon \mathbf{e}, \varepsilon \tilde{\mathbf{e}})_{L^2(T)} \} \\ &\quad + \sum_{F \in \mathbb{F}_h} h_F \{ ([[\mathbf{h} \times \mathbf{n}], [[\tilde{\mathbf{h}} \times \mathbf{n}]])_{L^2(F)} + ([[\mu \mathbf{h} \cdot \mathbf{n}], [[\mu \tilde{\mathbf{h}} \cdot \mathbf{n}]])_{L^2(F)} \\ &\quad \quad + ([[\mathbf{e} \times \mathbf{n}], [[\tilde{\mathbf{e}} \times \mathbf{n}]])_{L^2(F)} + ([[\varepsilon \mathbf{e} \cdot \mathbf{n}], [[\varepsilon \tilde{\mathbf{e}} \cdot \mathbf{n}]])_{L^2(F)} \}. \end{aligned}$$

The form is obviously symmetric and the above inequalities imply that

$$\|\mathbf{h}\| + \|\mathbf{e}\| \leq C b_{h,\omega}(\mathbf{h}, \mathbf{e}; \mathbf{h}, \mathbf{e}).$$

Hence (3.12) has a unique solution, provided that  $\lambda = -i\omega$  is not a Maxwell eigenvalue.

**3.3. Error estimates.** Let  $\{\Omega_i\}$  be a non-overlapping decomposition of  $\Omega$  corresponding to the different materials (i.e.  $\varepsilon$  and  $\mu$  are constants on each  $\Omega_i$ ). The space  $\widehat{\mathbf{H}}^s(\Omega) = \bigoplus \mathbf{H}^s(\Omega_i)$  consists of vector fields  $\mathbf{v} \in \mathbf{L}^2(\Omega)$  such that  $\mathbf{v}_i = \mathbf{v}|_{\Omega_i} \in \mathbf{H}^s(\Omega_i)$ . This is a Hilbert space with a norm

$$\|\mathbf{v}\|_s^2 = \sum \|\mathbf{v}_i\|_{\mathbf{H}^s(\Omega_i)}^2.$$

In this subsection, we assume that  $X_h$  is an approximation of  $X$  in the sense that

$$(3.13) \quad \inf_{x_h \in X_h} \|x - x_h\| \leq C h^s \|x\|_s \quad \text{for all } x \in \widehat{\mathbf{H}}^s(\Omega) \times \widehat{\mathbf{H}}^s(\Omega),$$

and any  $s \in (0, 1]$ . Here,  $h$  is the maximal diameter of an element in  $\mathbb{T}_h$ .

Additionally, we assume the following continuous embeddings

$$(3.14) \quad \mathbf{X}_1(\mu), \mathbf{X}_2(\varepsilon) \hookrightarrow \widehat{\mathbf{H}}^s(\Omega).$$

The embedding of  $\mathbf{X}_1(\mu)$  and  $\mathbf{X}_2(\varepsilon)$  in  $\mathbf{H}^s(\Omega)$  have been discussed in [24, 2, 10]. However, we prefer the regularity assumption (3.14), since for  $s > \frac{1}{2}$ , we have  $\mathbf{X}_1(\mu), \mathbf{X}_2(\varepsilon) \hookrightarrow \mathbf{H}^s(\Omega)$  only when  $\varepsilon$  and  $\mu$  are continuous.

Below we prove an estimate for the approximation error of each of the methods from the previous two subsections.

**Theorem 3.2.** *Let  $s \in [0, 1]$  be such that (3.13) and (3.14) hold. Assume that  $\lambda = -i\omega \neq 0$  is not an eigenvalue, and let  $(\mathbf{h}, \mathbf{e})$  be the solution of the time-harmonic problem with data  $\mathbf{j} \in \mathbf{H}(\text{div})$ ,  $\mathbf{m} \in \mathbf{H}_0(\text{div})$  and  $\rho$  and  $q$  defined by (2.22). Let  $(\mathbf{h}_h, \mathbf{e}_h)$  be the least-squares approximation obtained by either of the methods presented in the previous two subsections (for the method based on form modification assume  $s \neq \frac{1}{2}$ ). Then we have the error estimate*

$$\|\mathbf{h} - \mathbf{h}_h\| + \|\mathbf{e} - \mathbf{e}_h\| \leq C h^s \left( \|\mathbf{j}\|_{\mathbf{H}(\text{div})} + \|\mathbf{m}\|_{\mathbf{H}(\text{div})} \right),$$

where  $C > 0$  depends on  $\mu$ ,  $\varepsilon$ , and  $\omega$ , but is independent of  $h$ .

*Proof.* The result for the method using discrete inf-sup condition is a straightforward corollary from the quasi-optimality property (3.5) and the stability estimate (2.23) in Theorem 2.2. Indeed, combining (3.13) and (3.5), we get

$$\|\mathbf{h} - \mathbf{h}_h\| + \|\mathbf{e} - \mathbf{e}_h\| \leq C h^s (\|\mathbf{h}\|_s + \|\mathbf{e}\|_s).$$

On the other hand, (3.14) and (2.23) imply

$$\|\mathbf{h}\|_s + \|\mathbf{e}\|_s \leq C (\|\mathbf{h}\|_{\mathbf{X}_1(\mu)} + \|\mathbf{e}\|_{\mathbf{X}_2(\varepsilon)}) \leq C (\|\mathbf{j}\|_{\mathbf{H}(\text{div})} + \|\mathbf{m}\|_{\mathbf{H}(\text{div})}).$$

The error estimate in the theorem follows from the above two results.

We next consider the method based on form modification in the case  $s < \frac{1}{2}$ . The result follows by interpolation similar to the one in [5]. Specifically, for any  $x = (\mathbf{h}, \mathbf{e}) \in X$ , let  $x_h = (\mathbf{h}_h, \mathbf{e}_h) \in X_h$  be the solution of (3.12) with  $\mathbf{j}, \mathbf{m}, q$  and  $\rho$  defined by (2.11). Then,

$$\begin{aligned} C \|x_h\|^2 &\leq b_{h,\omega}(x_h; x_h) \\ &= (\mathbf{curl}_1 \mathbf{h} - \omega \varepsilon \mathbf{e}, \mathbf{curl}_{1,\omega}^h x_h)_{\mathbf{V}_{h,1}^*} + (\mathbf{curl}_2 \mathbf{e} - \omega \mu \mathbf{h}, \mathbf{curl}_{2,\omega}^h x_h)_{\mathbf{V}_{h,2}^*} \\ &\quad + (\text{div}_{1,\mu} \mathbf{h}, \text{div}_{1,\mu}^h \mathbf{h}_h)_{H_{h,1}^*} + (\text{div}_{2,\varepsilon} \mathbf{e}, \text{div}_{2,\varepsilon}^h \mathbf{e}_h)_{H_{h,2}^*} \leq C \|x_h\| \|x\|. \end{aligned}$$

Therefore,

$$(3.15) \quad \|x - x_h\| \leq C \|x\| \quad \text{for all } x \in X.$$

Let  $x$  be in  $\widehat{\mathbf{H}}_0^1(\Omega) \times \widehat{\mathbf{H}}_0^1(\Omega)$  where  $\widehat{\mathbf{H}}_0^1(\Omega) = \bigoplus \mathbf{H}_0^1(\Omega_i)$  and set  $\xi_h = (\tilde{\mathbf{h}}_h, \tilde{\mathbf{e}}_h)$  to be its  $\mathbf{L}^2(\Omega)$ -projection onto  $X_h$ . Then

$$\begin{aligned} C \|x_h - \xi_h\|^2 &\leq b_{h,\omega}(x_h; x_h - \xi_h) - b_{h,\omega}(\xi_h; x_h - \xi_h) \\ &= (\mathbf{curl}_1 \delta \mathbf{h} - \omega \varepsilon \delta \mathbf{e}, \mathbf{curl}_{1,\omega}^h \delta x_h)_{\mathbf{V}_{h,1}^*} \\ &\quad + (\mathbf{curl}_2 \delta \mathbf{e} - \omega \mu \delta \mathbf{h}, \mathbf{curl}_{2,\omega}^h \delta x_h)_{\mathbf{V}_{h,2}^*} \\ &\quad + (\text{div}_{1,\mu} \delta \mathbf{h}, \text{div}_{1,\mu}^h \delta \mathbf{h}_h)_{H_{h,1}^*} + (\text{div}_{2,\varepsilon} \delta \mathbf{e}, \text{div}_{2,\varepsilon}^h \delta \mathbf{e}_h)_{H_{h,2}^*} \\ (3.16) \quad &- \omega^2 \sum_{T \in \mathbb{T}_h} h_T^2 \{ (\mu \tilde{\mathbf{h}}_h, \mu \delta \mathbf{h}_h)_{\mathbf{L}^2(T)} + (\varepsilon \tilde{\mathbf{e}}_h, \varepsilon \delta \mathbf{e}_h)_{\mathbf{L}^2(T)} \} \\ &+ \sum_{F \in \mathbb{F}_h} h_F \{ ([[\delta \mathbf{h} \times \mathbf{n}]], [[\delta \mathbf{h}_h \times \mathbf{n}]])_{\mathbf{L}^2(F)} + ([[\mu \delta \mathbf{h} \cdot \mathbf{n}]], [[\mu \delta \mathbf{h}_h \cdot \mathbf{n}]])_{\mathbf{L}^2(F)} \\ &\quad + ([[\delta \mathbf{e} \times \mathbf{n}]], [[\delta \mathbf{e}_h \times \mathbf{n}]])_{\mathbf{L}^2(F)} + ([[\varepsilon \delta \mathbf{e} \cdot \mathbf{n}]], [[\varepsilon \delta \mathbf{e}_h \cdot \mathbf{n}]] )_{\mathbf{L}^2(F)} \}, \end{aligned}$$

where  $\delta x = (\delta \mathbf{h}, \delta \mathbf{e}) = x - \xi_h$  and  $\delta x_h = (\delta \mathbf{h}_h, \delta \mathbf{e}_h) = x_h - \xi_h$ .

Using standard inequalities and the special choice of  $\xi_h$ , we get

$$C \|x_h - \xi_h\| \leq \|x - \xi_h\| + h \|x\|_1,$$

which, together with (3.13), implies

$$(3.17) \quad \|x - x_h\| \leq C h \|x\|_1 \quad \text{for all } x \in \widehat{\mathbf{H}}_0^1(\Omega).$$

By interpolation between (3.15) and (3.17), we get that  $\|x - x_h\| \leq C h^s \|x\|_s$  for all  $x \in \widehat{\mathbf{H}}_0^s(\Omega) \times \widehat{\mathbf{H}}_0^s(\Omega)$ , where  $\widehat{\mathbf{H}}_0^s(\Omega) = \bigoplus \mathbf{H}_0^s(\Omega_i)$ . Since  $\widehat{\mathbf{H}}_0^s(\Omega) = \widehat{\mathbf{H}}^s(\Omega)$  when  $s < \frac{1}{2}$ , this is enough to prove the desired error estimate.

The proof can be extended to the case  $s > \frac{1}{2}$  if we estimate the boundary jump terms more carefully. Let  $\widehat{T}$  denote the reference element. The trace operator extends from smooth functions to a bounded operator from  $\mathbf{H}^s(\widehat{T})$  to  $\mathbf{L}^2(\partial\widehat{T})$  from which we have

$$(3.18) \quad C h_T \left( \|\mathbf{v} \cdot \mathbf{n}\|_{\mathbf{L}^2(\partial T)}^2 + \|\mathbf{v} \times \mathbf{n}\|_{\mathbf{L}^2(\partial T)}^2 \right) \leq \|\mathbf{v}\|_{\mathbf{L}^2(T)}^2 + h_T^{2s} |\mathbf{v}|_{\mathbf{H}^s(T)}^2$$

for any  $\mathbf{v} \in \mathbf{H}^s(T)$ ,  $s > \frac{1}{2}$  and  $T \in \mathbb{T}_h$ .

Let  $x = (\mathbf{h}, \mathbf{e})$  be in  $\mathbf{X}_1(\mu) \times \mathbf{X}_2(\varepsilon)$  and assume that (3.14) holds with  $s > 1/2$ . Then,

$$\llbracket \mathbf{h} \times \mathbf{n} \rrbracket_{\mathbf{L}^2(F)} = \llbracket \mathbf{e} \times \mathbf{n} \rrbracket_{\mathbf{L}^2(F)} = \llbracket \mu \mathbf{h} \cdot \mathbf{n} \rrbracket_{\mathbf{L}^2(F)} = \llbracket \varepsilon \mathbf{e} \cdot \mathbf{n} \rrbracket_{\mathbf{L}^2(F)} = 0$$

for any face  $F$ . Thus, (3.16) holds for  $x$ . We can estimate the terms in the sum over the faces using (3.18). The remaining terms are bounded as before and we get

$$C \|x_h - \xi_h\| \leq \|x - \xi_h\| + \sum_{T \in \mathbb{T}_h} \left[ h_T^s |x|_{\mathbf{H}^s(T)} + h_T \|x\|_{\mathbf{L}^2(T)} \right],$$

where we used the fact that  $|\xi_h|_{\mathbf{H}^s(T)} = 0$ . The result of the theorem follows from this estimate and (3.13).  $\square$

#### 4. NUMERICAL EXPERIMENTS

In this section, we report the results of some numerical experiments which illustrate the theory developed in the rest of the paper. For ease of implementation, we assume that the fields are real, i.e. we are solving the problem described in Remark 2.2. We also concentrate on the least-squares method from Section 3.1.

In all of our examples, we partition the domain  $\Omega$  into a shape regular mesh. For the components of  $X_h$ , we used piecewise constant vectors. The spaces composing  $Y_h$  are defined as piecewise linear and continuous functions enriched by face and element bubble functions as discussed earlier. The preconditioner for  $\mathcal{T}_{Y_h}$  is implemented by a multiplicative, two-level algorithm involving Gauss-Seidel smoothing on the bubble nodes and an exact solve or multigrid V-cycle on the piecewise linear subspace.

We first report computations on two-dimensional problems. Specifically, we consider a transverse electric (TE) mode where the geometry of the device is infinite along the  $z$ -axis, with an electric field pointing parallel to it. The magnitude of the electric field,  $\mathbf{e}_{3d}$ , is denoted by  $e$  and the magnetic field vector  $\mathbf{h}_{3d}$  is assumed to be orthogonal to the  $z$ -axis, i.e.,  $\mathbf{e}_{3d} = (0, 0, e)$  and  $\mathbf{h}_{3d} = (h_1, h_2, 0)$ . Due to the symmetry, the systems (2.6) and (2.7) reduce to problems in the cross-section domain  $\Omega$  in the  $xy$ -plane involving the unknowns  $\mathbf{h}(x, y) = (h_1(x, y), h_2(x, y))$  and  $e(x, y)$ . The right-hand side is given by

$\mathbf{j}_{3d} = (0, 0, j)$  and  $\mathbf{m}_{3d} = (m_1, m_2, 0)$ , where  $j \in L^2(\Omega)$  and  $\mathbf{m} = (m_1, m_2) \in \mathbf{H}_0(\text{div}; \Omega)$ . After integration by parts we get

$$\begin{cases} \langle \mathbf{curl}_1 \mathbf{h} - \omega \varepsilon e, w \rangle & \equiv (\mathbf{h}, \nabla \times w) - \omega (\varepsilon e, w) = (j, w) & \text{for all } w \in V_1 \equiv H_0^1(\Omega), \\ \langle \mathbf{curl}_2 e - \omega \mu \mathbf{h}, \mathbf{v} \rangle & \equiv (e, \nabla \times \mathbf{v}) - \omega (\mu \mathbf{h}, \mathbf{v}) = (\mathbf{m}, \mathbf{v}) & \text{for all } \mathbf{v} \in \mathbf{V}_2 \equiv \mathbf{H}^1(\Omega), \\ \langle \text{div}_{1,\mu} \mathbf{h}, \psi \rangle & \equiv -(\mu \mathbf{h}, \nabla \psi) = \omega^{-1} (\nabla \cdot \mathbf{m}, \psi) & \text{for all } \psi \in H_1 \equiv H^1(\Omega). \end{cases}$$

Here,  $\nabla \times \mathbf{v} = \partial_x \mathbf{v}_2 - \partial_y \mathbf{v}_1$  and  $\nabla \times w = (\partial_y w, -\partial_x w)$ . Note that

$$\nabla \times \mathbf{h}_{3d} = (0, 0, \nabla \times \mathbf{h}), \quad \nabla \times \mathbf{e}_{3d} = (\nabla \times e, 0), \quad \nabla \cdot \mathbf{h}_{3d} = \nabla \cdot \mathbf{h}, \quad \text{and } \nabla \cdot \mathbf{e}_{3d} = 0.$$

Often, in the literature, the magnetic field  $\mathbf{h}$  is eliminated from the original system, which leads to a second order problem for  $e \in H_0^1(\Omega)$ . Assuming that  $\varepsilon$  and  $\mu$  are constants, this problem is the Helmholtz equation

$$(4.1) \quad -\Delta e - \varepsilon \mu \omega^2 e = \omega \mu j + \nabla \times \mathbf{m}.$$

The development in Sections 2 and 3 extends naturally to the present situation. In particular, we have the above weak formulation which is based on the operator

$$\|B_{2d,\omega}(\mathbf{h}, e)\|^2 = \|\mathbf{curl}_1 \mathbf{h} - \omega \varepsilon e\|_{V_1^*}^2 + \|\mathbf{curl}_2 e - \omega \mu \mathbf{h}\|_{\mathbf{V}_2^*}^2 + \|\text{div}_{1,\mu} \mathbf{h}\|_{H_1^*}^2.$$

As in the three-dimensional case, we see that both least-squares methods from Section 3 are well posed, provided that  $\omega$  is not an eigenvalue.

As a first illustration, we consider an example involving a known smooth solution. We let  $\Omega$  be the unit square and take constant  $\mu$ ,  $\varepsilon$  and  $\omega$ . We set  $\mathbf{m}$  and  $j$  so that the solution is given by

$$(4.2) \quad \mathbf{h} = \nabla(\cos(\pi x) \cos(\pi y)), \quad e = x(1-x) \sin(\pi y).$$

We use a regular mesh of triangles obtained by first partitioning the square into  $n \times n$  equal smaller squares and then dividing each smaller square in two by the positive sloping diagonal. This initial mesh is uniformly refined, and on each level we use a diagonally preconditioned conjugate gradient algorithm (CG) to solve (3.4). The iterations are stopped when the residual norm is reduced by six orders of magnitude.

$h$	$\ (\mathbf{h}, e)\ _0$	$\varrho$	$n_{it}$	$N$	$time$
0.125	0.57762		9	384	0.01
0.0625	0.29090	1.9856	9	1536	0.06
0.03125	0.14571	1.9964	9	6144	0.21
0.015625	0.07289	1.9992	9	24576	0.92
0.0078125	0.03645	1.9998	9	98304	4.88
0.00390625	0.01822	2.0000	9	393216	24.8

TABLE 4.1. Numerical results for a two-dimensional problem with known smooth solution,  $\mu = \varepsilon = \omega = 1$ . Exact subspace solver.

We first set  $\mu = \varepsilon = \omega = 1$ . The numerical results for the two different subspace solvers are given in Table 4.1 and Table 4.2. We report the mesh size  $h$ , the approximation error in  $\mathbf{L}^2(\Omega) \times L^2(\Omega)$ , the ratio  $\varrho$  to the error on the previous grid, the number of conjugate gradient iterations  $n_{it}$ , the size of the system  $N$  and the computational time  $time$  (on a Dell Precision 650 workstation).

$h$	$\ (\mathbf{h}, e)\ _0$	$\varrho$	$n_{it}$	$N$	$time$
0.125	0.57762		9	384	0.01
0.0625	0.29091	1.9855	11	1536	0.02
0.03125	0.14572	1.9965	12	6144	0.09
0.015625	0.07289	1.9992	12	24576	0.37
0.0078125	0.03645	1.9998	12	98304	1.97
0.00390625	0.01822	2.0000	12	393216	10.2

TABLE 4.2. Numerical results for a two-dimensional problem with known smooth solution,  $\mu = \varepsilon = \omega = 1$ . Subspace solver using multigrid.

Our first observation is that the error behavior in  $\mathbf{L}^2(\Omega) \times L^2(\Omega)$  clearly illustrates the expected first order convergence rate. In all cases, the number of iterations required to reduce the residual by a factor of  $10^{-6}$  remains bounded independently of the number of unknowns. Note also, that using the multigrid preconditioner, instead of the exact solver, leads to a modest increase of the number of iterations while significantly reducing the overall solution time.

We also present results for the multigrid subspace solver when no element bubbles are used in the vector test space  $\mathbf{V}_2$  (i.e. we use the test space from [5]) in Table 4.3.

$h$	$\ (\mathbf{h}, e)\ _0$	$\varrho$	$n_{it}$	$N$	$time$
0.125	0.57812		9	384	0.01
0.0625	0.29134	1.9843	11	1536	0.02
0.03125	0.14599	1.9956	12	6144	0.07
0.015625	0.07302	1.9993	12	24576	0.31
0.0078125	0.03645	1.9999	12	98304	1.61
0.00390625	0.01826	2.0000	12	393216	8.25

TABLE 4.3. Numerical results for a two-dimensional problem with known smooth solution,  $\mu = \varepsilon = \omega = 1$ . Subspace solver using multigrid. No element bubbles in  $\mathbf{V}_2$ .

The increase in the approximation error is very small, especially compared to the reduction in the running time and the memory use. Thus, it seems that the element bubbles are an unnecessary overhead for this problem. In fact, this is typical for all the experiments that we conducted. Currently, we do not have a theoretical explanation for this behavior.

Next we investigate the behavior of our method in a neighborhood of an eigenvalue. This is done in Figure 2, where we set  $\mu = \varepsilon = 1$  and let  $\omega$  take values close to the first Maxwell eigenvalue  $\sqrt{2}\pi$ . For each such value of  $\omega$ , on the left we report the number of iterations, and on the right we plot the approximation error on each level. Different refinement levels are plotted consecutively, from coarse to fine, using the different colors given in the legend.

From these graphs one can observe that the change in  $\omega$  affects the number of iterations in a greater degree than the approximation error. It is also evident that when  $\omega = 4.4$ ,

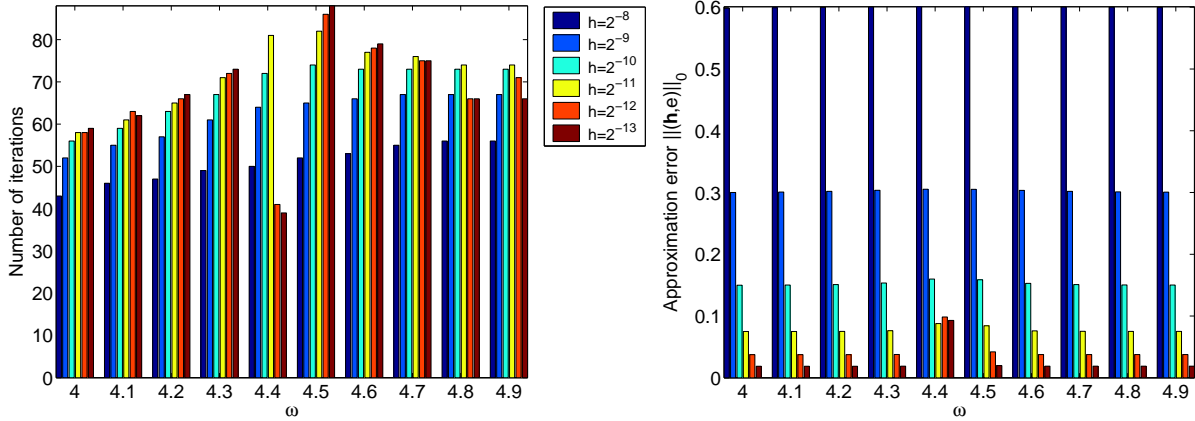


FIGURE 2. Convergence behavior and approximation error in a neighborhood of the eigenvalue  $\omega = \sqrt{2}\pi \approx 4.4$ . Here  $\mu = \varepsilon = 1$ .

parts of the eigenfunctions enter the computations on the last two levels and, even though the CG iterations converge fast, the approximation error increases. This is a numerical confirmation that values of  $\omega$  close to an eigenvalue should be avoided. We also note that the method works well for values of  $\omega$  in the interval  $[4.6, 4.9]$ , where the second order problem (4.1) is indefinite.

We conclude the experiments on the unit square by further investigating the effect of changing the parameters  $\omega$ ,  $\varepsilon$  and  $\mu$ . This is motivated by some applications, e.g. mixed digital and analog signal packages, where one needs an algorithm with convergence estimates that are independent of the frequency  $\omega$ . In [12], such results were obtained for the case of  $\omega$  in a neighborhood of zero. The approach there uses a mixed formulation with a “dummy” Lagrange multiplier (one that is identically zero). Further results in this direction are given in [19], where a FOSLS method is applied to the scalar Helmholtz equation with exterior radiation boundary conditions. The convergence of the resulting multigrid algorithm is uniform with respect to the wave number  $\omega$ , under the assumption that the domain is convex or has a smooth boundary.

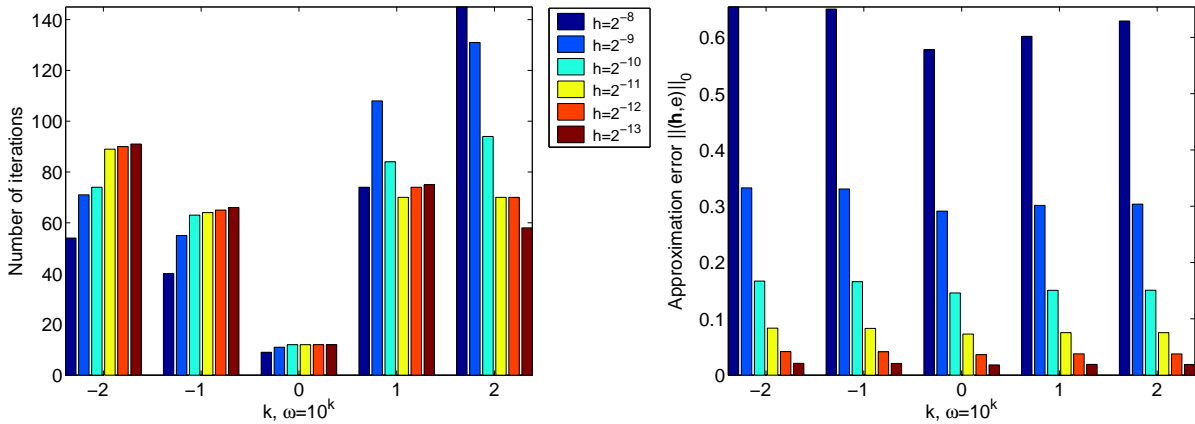


FIGURE 3. Convergence behavior and approximation error for a range of values  $\omega \in \{0.01, 0.1, 1, 10, 100\}$ . Here  $\mu = \varepsilon = 1$ .

Results illustrating the dependence on the electromagnetic coefficients are given in Figures 4 and 5.

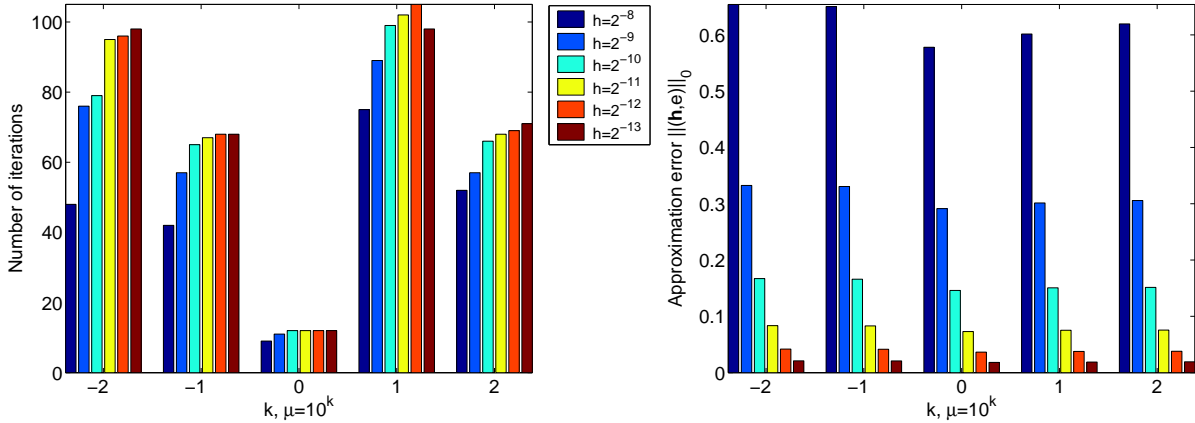


FIGURE 4. Convergence behavior and approximation error for a range of values  $\mu \in \{0.01, 0.1, 1, 10, 100\}$ . Here  $\omega = \varepsilon = 1$ .

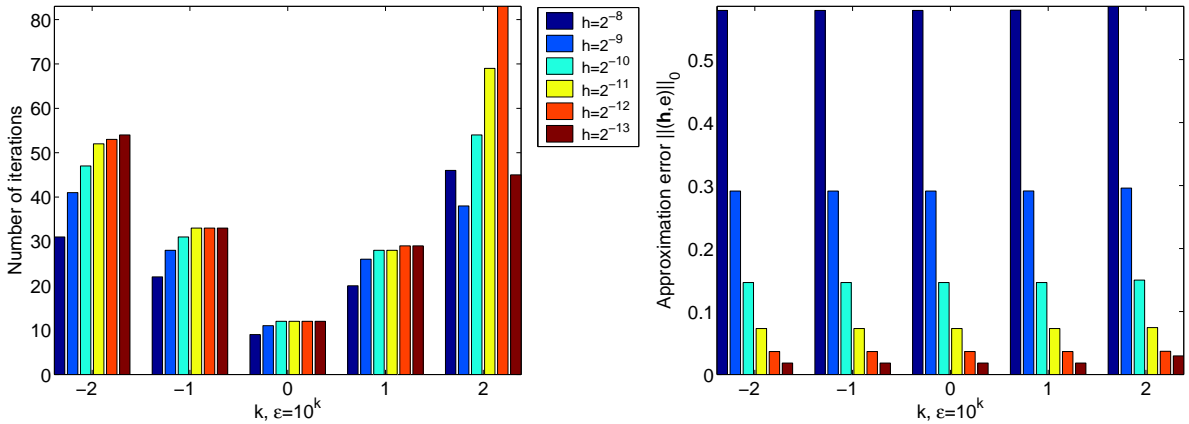


FIGURE 5. Convergence behavior and approximation error for a range of values  $\varepsilon \in \{0.01, 0.1, 1, 10, 100\}$ . Here  $\mu = \omega = 1$ .

Our second example is posed on the  $\Gamma$ -shaped domain  $\Omega = [-1, 1]^2 \setminus ([0, 1] \times [-1, 0])$ . We let  $\varepsilon = \mu = \omega = 1$  and set the problem such that the solution in polar coordinates is given by

$$e(\rho, \theta) = \rho^\beta \cos(\beta\theta) \quad \text{and} \quad \mathbf{h} = \nabla \times e, \quad \text{with} \quad \beta = \frac{2}{3}.$$

Note that, while  $e$  is in  $H^1(\Omega)$ ,  $\mathbf{h}$  is only in  $\mathbf{H}^s(\Omega)$  for  $s < \frac{2}{3}$ .

In Table 4.4, we present the results obtained with the least-squares solver based on multigrid and using no element bubbles in the vector test space. We report the level of uniform refinement  $\ell$ , the  $L^2(\Omega)$  error for  $\mathbf{h}$  with the ratio to the error on the previous grid, the  $L^2(\Omega)$  error for  $e$  with the same ratio, the number of iterations  $n_{it}$ , and the size of the problem  $N$ .

The number of iterations in Table 4.4 is constant across the levels of refinement as in the previous example. We also get the expected convergence rates—first order for  $e$  and

$\ell$	$\ \mathbf{h}\ _0$	$\varrho$	$\ e\ _0$	$\varrho$	$n_{it}$	$N$
0	0.78533		0.88500		9	12
1	0.51683	1.5195	0.44849	1.9733	12	48
2	0.33881	1.5254	0.22619	1.9828	12	192
3	0.21854	1.5503	0.11351	1.9927	12	768
4	0.13981	1.5631	0.05684	1.9969	12	3072
5	0.08901	1.5708	0.02844	1.9987	12	12288
6	0.05649	1.5756	0.01423	1.9994	12	49152
7	0.03579	1.5787	0.00711	1.9996	12	196608
8	0.02264	1.5806	0.00356	1.9996	12	786432

TABLE 4.4. Numerical results for the two-dimensional  $\Gamma$ -shaped domain. Subspace solver using multigrid. No element bubbles in  $\mathbf{V}_2$ .

order  $\frac{2}{3}$  for  $\mathbf{h}$  (which corresponds to a reduction factor of  $2^{2/3} \approx 1.587$ ). These results illustrate two properties of our method. First, we observe the optimal convergence rate for the low-regularity solution  $\mathbf{h}$ , and second, we allow for different orders of convergence for the electric and the magnetic field, depending on their smoothness. The latter is interesting, since it is not an obvious corollary from the estimate in Theorem 3.1.

The initial mesh together with the level lines of the computed approximations to the electric and magnetic fields are shown in Figure 6.

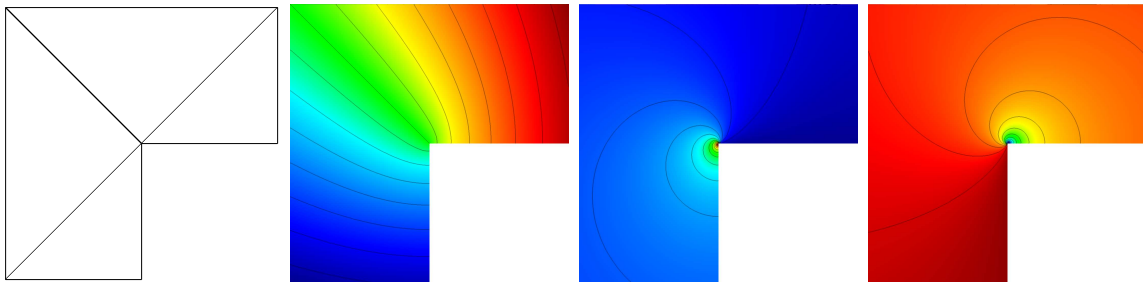


FIGURE 6. Two-dimensional problem in a  $\Gamma$ -shaped domain. The initial mesh and the approximations to  $e$ ,  $h_1$  and  $h_2$ .

Next we report computational examples in three dimensions. The implementation in this case is based on the form  $\mathcal{B}_\lambda$ , i.e. we are solving simultaneously the two real problems mentioned in Remark 2.4.

For our first 3D test we let  $\Omega = [0, 1]^3$  and set  $\varepsilon = \mu = \omega = 1$ . We discretize with a sequence of uniformly refined tetrahedral meshes. In this example, we choose the right-hand side data corresponding to the following smooth solution vectors:

$$\mathbf{h} = (f_3, -f_1, f_2) + i(3f_3, 4f_1, 5f_2) \quad \text{and} \quad \mathbf{e} = (2f_1, -f_2, f_3) + i(-f_1, 4f_2, f_3).$$

Here the scalar functions  $f_k$  are given by

$$\begin{aligned} f_1 &= \cos(\pi x) \sin(\pi y) \sin(\pi z), \\ f_2 &= \sin(\pi x) \cos(\pi y) \sin(\pi z), \\ f_3 &= \sin(\pi x) \sin(\pi y) \cos(\pi z). \end{aligned}$$

The rest of the setup is the same as in two dimensions.

$\ell$	$\ \Re(\mathbf{h})\ _0$	$\varrho$	$\ \Im(\mathbf{h})\ _0$	$\varrho$	$\ \Re(\mathbf{e})\ _0$	$\varrho$	$\ \Im(\mathbf{e})\ _0$	$\varrho$	$n_{it}$	$N$
1	0.30672		1.01236		0.38454		0.59629		21	1152
2	0.14402	2.13	0.55816	1.81	0.19970	1.93	0.33269	1.79	23	9216
3	0.06945	2.08	0.27983	1.99	0.09764	2.05	0.16744	1.98	22	73728
4	0.03438	2.02	0.13990	2.00	0.04852	2.01	0.08384	2.00	22	589824
5	0.01714	2.01	0.06993	2.00	0.02422	2.00	0.04193	2.00	22	4718592

TABLE 4.5. Numerical results for the unit cube. Subspace solver using multigrid.

The results obtained with the least-squares solver based on multigrid and using element bubbles in the vector test space are presented in Table 4.6. Employing similar notation as before, we report the level of uniform refinement, the  $L^2(\Omega)$  error for the real and imaginary part of both  $\mathbf{h}$  and  $\mathbf{e}$  together with the ratio to the error on the previous grid. We observe the expected first order convergence for each of the solution components. As in the previous test, we get a constant number of conjugate gradient iterations across the refinement levels.

$\ell$	$\ \Re(\mathbf{h})\ _0$	$\varrho$	$\ \Im(\mathbf{h})\ _0$	$\varrho$	$\ \Re(\mathbf{e})\ _0$	$\varrho$	$\ \Im(\mathbf{e})\ _0$	$\varrho$	$n_{it}$	$N$
1	0.30942		1.01940		0.39290		0.60185		21	1152
2	0.14473	2.14	0.56018	1.82	0.20087	1.96	0.33381	1.80	23	9216
3	0.06965	2.08	0.28060	1.99	0.09801	2.05	0.16794	1.99	22	73728
4	0.03447	2.02	0.14026	2.00	0.04867	2.01	0.08407	2.00	22	589824
5	0.01719	2.01	0.07012	2.00	0.02429	2.00	0.04205	2.00	22	4718592

TABLE 4.6. Numerical results for the unit cube. Subspace solver using multigrid. No element bubbles in  $\mathbf{V}_1$  and  $\mathbf{V}_2$ .

In Table 4.6 we repeat the same experiments using multigrid solver without element bubbles. The results are very similar to those in Table 4.5, with only a slight increase in the approximation error. Thus we confirm the observation made in 2D, that the element bubbles can be omitted without compromising the performance of the solver.

In contrast to the above results, we claim that the face bubbles are essential for good convergence. To demonstrate this, we again solve on the third and fourth level, but this time using test spaces with no bubble functions at all. When  $\ell = 3$ , this method converges after 136 iterations and results in the following approximation errors: 0.116, 0.413, 0.151 and 0.247. For  $\ell = 4$ , we need 263 iterations and the approximation errors are 0.055, 0.193, 0.076 and 0.124. These results are enough to conclude that the number of iterations increases significantly with the refinement level.

The next numerical illustration is posed on the three hexahedral approximations of the unit ball given in Figure 7. The same meshes were used in [4] for Maxwell eigenvalue computations. Even though these meshes are *non-nested*, their mesh sizes are related in a manner close to the one obtained through uniform refinement. Thus, we can think of them as three consecutive levels,  $\ell = 1, 2, 3$ , of discretization of the unit ball. This is

further supported by the results in Figure 4 from [4], which suggest that the eigenvalues computed on the meshes in Figure 7 converge to the eigenvalues of the unit ball. For example, the minimal eigenvalues for each of the three meshes were found to be 2.826, 2.761, and 2.748, while the minimal eigenvalue of the ball is approximately 2.744 (see Table 6.1 in [4]).

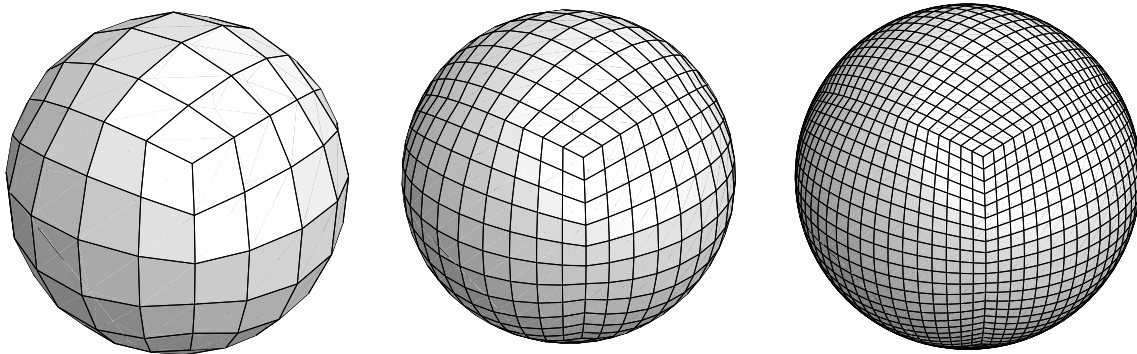


FIGURE 7. The sequence of meshes used for discretization of the unit ball.

To investigate the convergence behavior, we set up a problem with  $\mu = \varepsilon = \omega = 1$  and right-hand side corresponding to the following exact solutions on the unit ball

$$\mathbf{h} = (-y, x, 0) + i(0, -z, y) \quad \text{and} \quad \mathbf{e} = (x, y, z) - i(x, y, z).$$

We apply the least-squares algorithm and report the results in Table 4.7. For simplicity, we used exact subspace solver instead of multigrid in the definition of  $\mathcal{T}_{Y_n}$ . The notation is similar to before, but note that here the approximation error is computed against the above solutions and not against the (unknown) exact solution on the given level.

$\ell$	$\ \mathfrak{R}(\mathbf{h})\ _0$	$\varrho$	$\ \mathfrak{S}(\mathbf{h})\ _0$	$\varrho$	$\ \mathfrak{R}(\mathbf{e})\ _0$	$\varrho$	$\ \mathfrak{S}(\mathbf{e})\ _0$	$\varrho$	$n_{it}$	$N$
1	0.16674		0.16676		0.20461		0.20459		30	10500
2	0.07807	2.14	0.07807	2.14	0.09566	2.14	0.09566	2.14	36	111804
3	0.04112	1.90	0.04112	1.90	0.05037	1.90	0.05037	1.90	39	777924

TABLE 4.7. Numerical results for the unit ball. Exact subspace solver. No element bubbles in  $\mathbf{V}_1$  and  $\mathbf{V}_2$ .

The factor  $\varrho$  is in good agreement with the averaged mesh size ratios between different levels, which are 2.21 and 1.92. We can conclude that we get first order convergence and bounded number of iterations even in this somewhat unusual situation.

Finally, we use the same setup to investigate the behavior of the method in a neighborhood of an eigenvalue. We fix  $\mu = \varepsilon = 1$  and let  $\omega$  take values close to 2.744. For each such value in Figure 8, we graph the number of CG iterations (left plot) and the approximation error (right plot). As before, the different levels (corresponding to the meshes in Figure 7) are grouped together, from coarse to fine, using the colors in the legend.

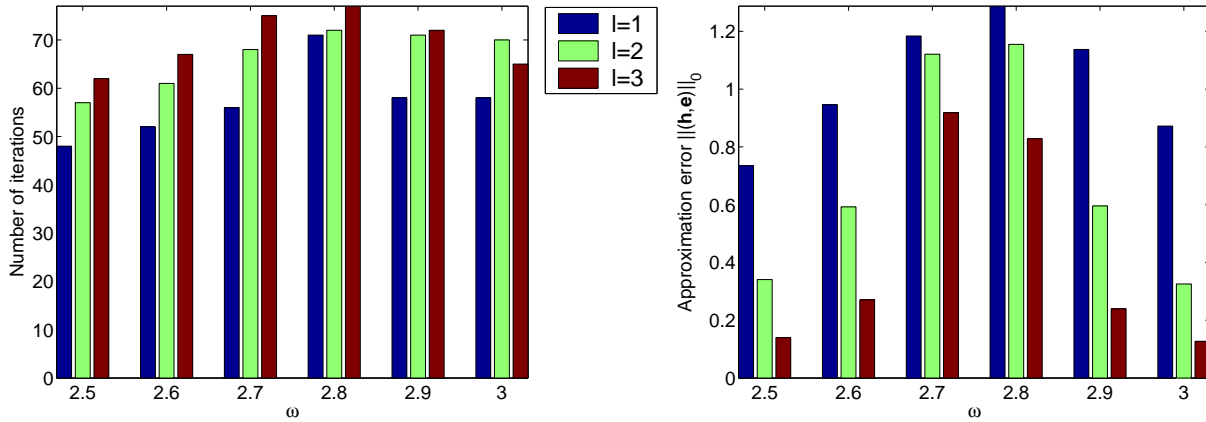


FIGURE 8. Convergence behavior and approximation error in a neighborhood of the eigenvalue  $\omega \approx 2.744$ . Here  $\mu = \varepsilon = 1$ .

These results are similar to the two-dimensional case presented in Figure 2. Again, when  $\omega \in \{2.7, 2.8\}$  the influence of the eigenfunctions leads to increased approximation error and the loss of first order convergence. This time, however, it also leads to an increased number of iterations. As before, the method works well for  $\omega \in \{2.9, 3\}$  when the corresponding curl-curl problem (2.3) is indefinite.

## 5. ACKNOWLEDGMENT

We would like to thank Veselin Dobrev for his contributions to the code used for the computations in Section 4.

## REFERENCES

- [1] R. A. Adams and J. F. Fournier. *Sobolev Spaces*, volume 140 of *Pure and Applied Mathematics*. Academic Press, Boston, 2003.
- [2] C. Amrouche, C. Bernardi, M. Dauge, and V. Girault. Vector potentials in three-dimensional nonsmooth domains. *Math. Methods Appl. Sci.*, 21(9):823–864, 1998.
- [3] F. Ben Belgacem, A. Buffa, and Y. Maday. The mortar method for the Maxwell’s equations in 3D. *C.R. Acad. Sci. Paris*, 329:903–908, 1999.
- [4] J. H. Bramble, T. V. Kolev, and J. E. Pasciak. The approximation of the Maxwell eigenvalue problem using a least-squares method. *Math. Comp.*, 2004. to appear.
- [5] J. H. Bramble and J. E. Pasciak. A new approximation technique for div-curl systems. *Math. Comp.*, 73(248):1739–1762, 2004.
- [6] P. Clément. Approximation by finite element functions using local regularization. *Rev. Française Automat. Informat. Recherche Opérationnelle Sér. Rouge Anal. Numér.*, 9(R-2):77–84, 1975.
- [7] M. Costabel. A remark on the regularity of solutions of Maxwell’s equations on Lipschitz domains. *MMAAS*, 12:365–368, 1990.
- [8] M. Costabel. A coercive bilinear form for Maxwell’s equations. *Jour. Math. Anal. Appl.*, 157(2):527–541, 1991.
- [9] M. Costabel and M. Dauge. Maxwell and Lamé eigenvalues on polyhedra. *Math. Methods Appl. Sci.*, 22(3):243–258, 1999.
- [10] M. Costabel, M. Dauge, and S. Nicaise. Singularities of Maxwell interface problems. *Modél. Math. Anal. Numér.*, 33(3):627–649, 1999.
- [11] L. Demkowicz, P. Monk, C. Schwab, and L. Vardapetyan. Maxwell eigenvalues and discrete compactness in two dimensions. Technical Report 99-12, TICAM, 1999.

- [12] L. Demkowicz and L. Vardapetyan. Modeling of electromagnetic absorption/scattering problems using *hp*-adaptive finite elements. *Comp. Meth. Appl. Mech. Eng.*, 152:103–124, 1998.
- [13] A.-S. B. Dhia, C. Hazard, and S. Lohrengel. A singular field method for the solution of Maxwell's equations in polyhedral domains. *SIAM J. Appl. Math.*, 59(6):2028–2044, 1999.
- [14] J. Gopalakrishnan, L. García-Castillo, and L. Demkowicz. Nédélec spaces in affine coordinates. *Computers and Mathematics with Applications*, 2005. to appear.
- [15] J. Gopalakrishnan and J. E. Pasciak. Overlapping Schwarz preconditioners for indefinite time harmonic Maxwell equations. *Math. Comp.*, 72(241):1–15, 2003.
- [16] R. Hiptmair. Multigrid method for Maxwell's equations. *SIAM J. Numer. Anal.*, 36(1):204–225, 1999.
- [17] R. Hiptmair and A. Toselli. Overlapping Schwarz methods for vector valued elliptic problems in three dimensions. In *Parallel solution of PDEs*, IMA Volumes in Mathematics and its Applications. Springer-Verlag, Berlin, 1998.
- [18] J.-M. Jin. *The Finite Element Method in Electromagnetics*. John Wiley & Sons, New York, 2002.
- [19] B. Lee, T. A. Manteuffel, S. F. McCormick, and J. Ruge. First-order system least-squares for the Helmholtz equation. *SIAM J. Sci. Comp.*, 21(5):1927–1949, 2000.
- [20] P. Monk. *Finite Element Methods for Maxwell's Equations*. Numerical Mathematics and Scientific Computation. Oxford University Press, Oxford, UK, 2003.
- [21] J.-C. Nédélec. Mixed finite elements in  $\mathbb{R}^3$ . *Numer. Math.*, 35:315–341, 1980.
- [22] J.-C. Nédélec. A new family of mixed finite elements in  $\mathbb{R}^3$ . *Numer. Math.*, 50:57–81, 1986.
- [23] I. Perugia, D. Schötzau, and P. Monk. Stabilized interior penalty methods for the time-harmonic Maxwell equations. *Comp. Meth. Appl. Mech. Eng.*, 191:4675–4697, 2002.
- [24] J. Saranen. On an inequality of Friedrichs. *Math. Scand.*, 51:310–322, 1982.
- [25] L. R. Scott and S. Zhang. Finite element interpolation of nonsmooth functions satisfying boundary conditions. *Math. Comp.*, 54(190):483–493, 1990.
- [26] A. Toselli. Overlapping Schwarz methods for Maxwell's equations in three dimensions. Technical Report 736, Courant Institute of Mathematical Sciences, New York, June 1997.
- [27] F. T. Ulaby. *Fundamentals of Applied Electromagnetics*. Prentice Hall, Upper Saddle River, NJ, 2000.
- [28] J. L. Volakis, A. Chatterjee, and L. C. Kempel. *Finite Element Method for Electromagnetics : Antennas, Microwave Circuits, and Scattering Applications*. IEEE Press, New York, 1998.
- [29] C. Wolfe, U. Navsariwala, and S. Gedney. A parallel finite-element tearing and interconnecting algorithm for solution of the vector wave equation with PML absorbing medium. *IEEE Transactions on Antennas and Propagation*, 47:278–284, 2000.

DEPARTMENT OF MATHEMATICS, TEXAS A&M UNIVERSITY, COLLEGE STATION, TX 77843-3368.

*E-mail address:* `bramble@math.tamu.edu`

CENTER FOR APPLIED SCIENTIFIC COMPUTING, LAWRENCE LIVERMORE NATIONAL LABORATORY, P.O. BOX 808, L-551, LIVERMORE, CA 94551.

*E-mail address:* `tzanio@llnl.gov`

DEPARTMENT OF MATHEMATICS, TEXAS A&M UNIVERSITY, COLLEGE STATION, TX 77843-3368.

*E-mail address:* `pasciak@math.tamu.edu`